Energetics and Mechanics of Humans Running on Surfaces of Different Compliance

by

Amy Elizabeth Kerdok

B.S., Biomedical Engineering (1997)

Rensselaer Polytechnic Institute

Submitted to the Department of Mechanical Engineering
in Partial Fulfillment of the Requirements for the Degree of

Master of Science in Mechanical Engineering

at the

Massachusetts Institute of Technology

September 1999

Signature of Author.....
Department of Mechanical Engineering
August 12, 1999

Certified By.....
Hugh M. Herr, Ph.D.
Artificial Intelligence Laboratory
Thesis Supervisor

Certified By.....
Roger Kamm, Ph.D.
Professor of Mechanical Engineering
Departmental Reader

Accepted By.....
Ain A. Sonin
Chairman, Department Committee on Graduate Student

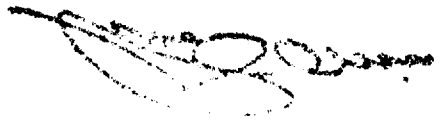

Energetics and Mechanics of Humans Running on Surfaces of Different Compliance

by

Amy Elizabeth Kerdok

Submitted to the Department of Mechanical Engineering
on August 12, 1999 in partial fulfillment of the
requirements for the Degree of Master of Science in
Mechanical Engineering

ABSTRACT

Running is a form of locomotion during which active muscles consume metabolic energy to support the weight of the runner, and elastic components (tendons, ligaments, muscles, and bones) conserve energy for the runner. In this thesis we studied both the energetics and mechanics of running on surfaces of different stiffness to try and further the understanding of the basic control mechanisms behind animal locomotion.

An experimental track with adjustable surface stiffness was designed and built to fit on a level treadmill surface. A force plate positioned beneath the track was used to measure vertical reaction forces. Eight male subjects (mean body mass 74.39 ± 7.12 kg; leg length 0.959 ± 0.049 m, mean ± S.D.) participated in an experiment where they ran at 3.7 m/s over five different surface stiffnesses (75.4, 97.5, 216.8, 454.2, and 945.7 kN/m) on the treadmill. Metabolic, force, and kinematic data were collected. We found that the runner's cost of transport (the amount of energy required to move a unit weight a unit distance) decreased by 12% over the 12-fold change in surface stiffness, and the leg stiffness of the runner increased by 29%. However, the total stiffness of the runner's leg plus the track remained constant as surface stiffness decreased. These results suggest that runners adjust leg stiffness to compensate for changes in surface stiffness while maintaining consistent running dynamics on all surfaces.

A mathematical model of the runner's leg was developed at each ground stiffness, to test the assumption that the leg, as a whole, behaves as a linear spring. The model was able to accurately reproduce the experimental data. We also used the model to test whether a constant leg stiffness would effect overall running dynamics. We found that if leg stiffness was not adjusted to compensate for the complaint surfaces, overall running dynamics change, which is contrary to the experimental results. This suggests that changing leg stiffness is a general mechanism of running necessary to maintain similar running dynamics on all ground surfaces.

Dedication

This thesis is dedicated to my advisor professor Thomas A. McMahon; the man whose ideas, energy, enthusiasm, guidance, and knowledge provided the foundation of not only this work, but also much of the work in the field of biomechanics as a whole. Thomas A. McMahon sadly and unexpectedly passed away in February 1999. To borrow the words from a fellow lab mate, he was not only a wonderful advisor and mentor, but also a friend. I wish he could have been able to physically witness the results of this work, because this is a topic he held close to his heart.

Acknowledgements

This thesis could not have been completed without the help of many people. In the wake of my advisor's (Thomas A. McMahon) tragic death, many people came forth to offer assistance of all kinds. Without the support from these people this work would never have been completed. To thank and acknowledge everyone would be impossible, but there are a select few I'd like to recognize whose efforts went above and beyond.

I'd first like to thank the Witaker Foundation. The funding I received from them allowed me to be a "free agent" to choose exactly what project interested me without having to worry about much additional funding.

Dr. Hugh M. Herr from the Massachusetts Institute of Technology's Leg Laboratory deserves more than a thank you for stepping up to take over the role of my primary research advisor after Dr. McMahon's death. Dr. Herr was an invaluable source of ideas, knowledge, and motivation. Similarly, Dr. Andrew Biewener from Harvard University's Concord Field Station provided me with infinite council and support. The time, space, equipment, and advice he provided made me feel as if I was one of his own graduate students, and I am most appreciative. Other people at the Concord Field station deserve a word of thanks for their assistance in my thesis as well. Mike Williamson was my extremely helpful and diligent assistant throughout my experiments, and Dr. Peter Weyand was not only a subject, but also a source of advice and technical help. Lastly, Seth Wright and Matthew Bellizzi were the technical support and masterminds behind my complicated LabView programs.

Outside help was also a critical component leading to the completion of this thesis. Dr. Claire T. Farley from the University of California, Berkely was a constant source of direction and expert knowledge in the area of running mechanics. Dr. Roger Kamm voluntarily became my thesis reader and provided me with valuable feedback. Members of the MIT Leg Laboratory as well as Harvard's and MIT's machine shops are credited for a lot of technical support and equipment use. Without the many volunteer subjects that chose to run in my experiment, this work would have been nothing but an interesting idea. I thank them for their time, their legs, and their great efforts, which helped to make this work a reality.

Finally, I'd like to recognize the people who had to deal with me on a daily basis. The women of the Harvard Biomechanic's Lab were patient with my questions, my mess, and my concerns. They provided me with a fun and supportive environment to work in and I'm grateful. I am also grateful to my family and friends, who believed in my abilities, listened to my problems, calmed my stresses, and supported my decisions. I'd especially like to extend my sincere thanks to Laura Chapman. She now knows more about running biomechanics than she probably ever cared to, but I couldn't have successfully completed this thesis without her intellectual and personal support, drawing talents, and motivation.

Thanks to all!

Table of Contents

List of Figures

Nomenclature

Dimensional variables

M_m	-	Mass of the runner
Δy_{com}	-	Vertical displacement of the runner's center of mass (com)
ΔL	-	Distance compressed by the leg spring
L_o	-	Leg length
θ	-	½ the Angle the leg sweeps through during ground contact
K_{leg}	-	Spring stiffness of the leg
K_{surf}	-	Spring stiffness of the running surface
D_{surf}	-	Vertical displacement of the track surface
M_{track}	-	Mass of the track surface
F_{grf}	-	Ground reaction force
K_{vert}	-	Effective vertical stiffness of the runner
W_b	-	Body weight
Y_{max}	-	Maximum deflection of a simply supported beam
F	-	Applied vertical force
L	-	Length of simply supported beam
E	-	Elastic (Young's) Modulus of a linearly plastic material
I	-	moment of inertia
FS	-	Factor of safety
σ_u	-	Ultimate stress for a material
σ_{max}	-	Maximum stress in a material
ω_d	-	Natural frequency
T_d	-	Period of oscillation
$\frac{d^2x}{dt^2}$	-	Acceleration in the x direction
F_{peak}	-	Peak vertical ground reaction force
t_c	-	Ground contact time
dur_{tot}	-	Stride time
freq	-	Stride (footprints of the same foot) frequency
Sl	-	Step (one foot to the next foot) length
Hz	-	Hertz (1/sec)
u_x	-	Forward speed (x direction)
Δy_{rel}	-	Relative displacement of the runner's center of mass
V_{tot}	-	Total volume of expired gas

$V_{I,f}$ - Initial and final volume respectively

$t_{sample,}$ - Sample time

$t_{collection}$ - Collection time

$P_{room,vapor}$ - Room and vapor pressure respectively

T_{gas} - Gas temperature

$\dot{V}O2$ - Rate of oxygen consumption

$\dot{V}CO2$ - Rate of carbon dioxide production

COT - Cost of transport

$K_{tot,L}$ - Overall stiffness of system

$K_{tot,V}$ - Overall vertical stiffness of system

C_o - Cost coefficient

E_{com} - Total mechanical energy of the runner's center of mass

E_{track} - Energy stored and returned in the track

E_{kf} - Forward kinetic energy

E_p - Gravitational potential energy

E_{kv} - Vertical kinetic energy

v_y - Vertical velocity of runner

w_y - Vertical velocity of track

F_x, F_y - Horizontal and vertical forces respectively

a_x, a_y - Horizontal and vertical accelerations respectively (also in $(\cdot\cdot)$ form)

F_{leg} - Force in the leg due to the leg spring

g - Gravitational acceleration (9.81 m/s^2)

t - Time

b - Damping coeffiecient

Dimensionless variables

$X_m = \frac{x_m}{L_o}$ - Horizontal position of the center of mass from the y axis

$Y_m = \frac{y_m}{L_o}$ - Vertical position of the center of mass from the undeflected track surface (y=0)

$Y_t = \frac{y_t}{L_o}$ - Vertical position of the track mass (negative) taken from the undeflected track surface (y=0)

$T = t\left(\frac{g}{L_o}\right)^{1/2}$ - Time

$$K_{LEG} = \frac{K_{leg} L_o}{M_m g} \quad -$$ Leg stiffness

$$M = \frac{M_m}{M_t} \quad -$$ Ratio of runner's mass to track mass

$$R = \frac{K_{surf}}{K_{leg}} \quad -$$ Ratio of surface stiffness to leg stiffness

$$B = \frac{b}{M_t \left(\frac{g}{L_o} \right)^{1/2}} \quad -$$ Dampening coefficient

$$U = \frac{u_x}{(gL_o)^{1/2}} \quad -$$ Horizontal velocity of runner

$$V = \frac{v_y}{(gL_o)^{1/2}} \quad -$$ Vertical velocity of runner

$$W = \frac{w_z}{(gL_o)^{1/2}} \quad -$$ Vertical velocity of track

Chapter 1
Introduction

1.1 Background

Locomotion has been studied for a long time, yet we are still trying to understand the mechanisms that allow animals to move gracefully and effectively over different terrain. The goal of this thesis is to study the biomechanics of human running and, more specifically, to understand the energetic and mechanical effects of running on surfaces of different compliance.

To many people, the thought of human running is one associated with fatigue and work. Perhaps this is the case because running is a costly process that requires metabolic energy. A person has to generate leg forces to support body weight and to accelerate forward. It is believed that the primary cost of running is the cost of supporting body weight throughout ground contact (Kram and Taylor, 1990). As a person runs faster, the foot is in contact with the ground for a shorter period of time, and the muscles must generate larger amounts of force. The larger force is obtained through the recruitment of faster and stronger muscle fiber types, which use more metabolic energy and have less endurance. Therefore, the cost is associated with the volume as well as the rate of force development of active muscles (Alexander, 1991; Biewener, 1990).

Despite the great costs associated with running, it is our fastest mode of natural transportation. Humans use many mechanisms to minimize the cost of running. It has been shown that the whole body operates at an efficiency of 40-50% during running (Cavagna et al., 1964). Since the maximum efficiency of contracting muscle is 25%, something else must contribute to the running process. It has been shown that the added contribution likely comes from the elastic recoil of muscle-tendon springs (Cavagna et al., 1964; Cavagna et al., 1977). Energy is conserved by the leg's elastic bounce storing mechanical energy during early stance and then recovering it near the end of stance (Cavagna et al., 1977). In fact, running is often likened to a bouncing rubber ball that moves forward and upward with each ground contact (Cavagna et al., 1964).

Where is energy stored in the leg? In other words, what are these muscle-tendon (leg) springs? Bones, muscles, tendons, and ligaments all stretch to some extent and together account for the leg spring (Cavagna et al., 1976). Muscle fibers can stretch elastically, but only by 3% before cross-bridges begin to cycle. The main components of the leg spring may be the tendons of the quadriceps and the Achilles tendon that can stretch by 8% before breaking, and the plantar ligaments of the foot (Alexander, 1992). Tendons in general return 93% of the work required to stretch them (Alexander, 1988; Alexander, 1992). The Achilles tendon alone accounts for 35% of the total energy return in a stride. The arch of the foot and it's ligaments have an energy return of 80% (Alexander, 1992). The stretching and deformation of these components allow for more work to be done

elastically, and therefore result in the muscles having to shorten less. This is beneficial because operating muscles isometrically allows for greater force generation at minimized cost (Taylor, 1992).

Researchers have found that treating the entire leg as a single linear spring serves quite well in representing the mechanics of the leg while in contact with the ground during running (Alexander, 1992; Farley et al., 1991; Farley et al., 1993; Farley and Morgenroth, 1999; Ferris and Farley, 1997; Ferris et al., 1998; He et al., 1991; McGeer, 1990; McMahon and Cheng, 1990; McMahon, 1990). The leg spring has since been studied both theoretically and experimentally under many different circumstances. Modeling the leg as a simple mass and linear spring has been a useful tool in predicting the experimental results of many studies. This model has also given insight into the general principles that govern the biomechanics of running. For instance, it was thought that running with a leg spring of constant stiffness was a basic and invariant principle of running (Farley et al., 1993). However, experimental data also supports that, although humans generally keep leg stiffness (K_{leg}) constant, leg stiffness can be altered to adjust for changes in limb posture, stride frequency, hopping height and surface stiffness (Farley et al., 1991; Ferris et al., 1998; McMahon and Greene, 1979; McMahon et al., 1987). Modeling these situations has shown that K_{leg} does have to be altered in order to maintain similar running dynamics and to avoid injury (Ferris et al, 1998).

1.2 Motivation

A main concept in understanding human running lies in understanding the ways humans try to minimize metabolic cost. Understanding this involves linking together many relationships of the mechanics and energetics of human running.

Researchers have looked at how a person's environment affects how they run. For instance, could a surface or a running shoe be altered in such a way as to increase the spring-like properties of the leg? How does a person adapt to changes in terrain? Running shoes have been tested and were found to be less important (returning only 60% of the energy) than the tendons and ligaments in the foot (Alexander, 1992). However, altering shoe design such that the midsole could stretch and recoil more like a spring would actually make shoes unstable, allowing for medial/lateral rocking. Consequently, shoes are designed to be stiffer than legs for safety reasons (Alexander, 1992; Clarke et al., 1983; Nigg et al., 1987).

McMahon and Greene took a different approach. They altered ground stiffness to understand its effects on running mechanics (1979). They compared running on ground stiffnesses ranging from an asphalt track to large pillows and found that at intermediate surface stiffnesses (giving roughly a 9mm deflection for a 70kg running man) running speed was enhanced compared to running speeds on a rigid asphalt track. This enhancement was defined as a combination of decreasing ground contact time, increasing step length, and decreasing initial peak ground reaction force. These changes resulted in an increase in running speed by 2-3% and a decrease in

running injuries by 50%. A primary assumption of the model that resulted from this work was that the leg spring was held at a constant stiffness over all surfaces. Recent studies have shown that K_{leg} does indeed change when running over surfaces of different stiffness (Ferris et al., 1998). Therefore the original model assumptions are perhaps incorrect. It is also not understood why a runner's performance is "enhanced" in the "tuned track" range. Lastly, what could be learned from reexamining running on surfaces of different stiffness from an energetics and mechanics perspective? Animals encounter many different ground surfaces; most of which don't store and return energy like the surfaces that are built in an experimental setting. Yet humans, and especially athletes, run on all types of surfaces including man made tracks. Can an experimental set up still be used to understand the overall mechanisms behind running in the "real world"?

1.3 Thesis Aims

Understanding human running is a challenge that has been tackled by many researchers. Relationships and mechanisms have been developed and tested to piece together theories on how humans run. In this thesis, we hoped to expand upon these theories and to link empirical relationships not yet established. We focused on the energetic as well as the mechanical effects of running on surfaces of different stiffness, including those stiffnesses that are in the range of the tuned track designed by McMahon and Greene (1979). We hypothesized that the metabolic cost of running is lowered when running on the compliant surfaces within the range of the tuned track, and that runners will adapt to these surfaces without altering their general running dynamics.

We tested our hypothesis by measuring the metabolic and mechanical parameters of human runners. Chapter 2 gives a detailed account of experimental methods and results. A spring-mass model was then developed to see if the assumption of representing the leg as a linear spring could predict the running behavior observed in the experiments. Chapter 3 provides all the modeling information and results. Lastly, Chapter 4 summarizes the primary results of the thesis and discusses future directions.

1.4 References

Alexander, R. M. (1988). Elastic Mechanisms in Animal Movement (Cambridge UK: Cambered University), pp. 30-50.

Alexander, R. M. (1991). Energy-Saving Mechanisms in Walking and Running. Journal of Experimental Biology *160*, 55-69.

Alexander, R. M. (1992). The Human Machine, R. M. Alexander, ed. (London: Natural History Museum Publications).

Alexander, R. M. (1992). A Model of Bipedal Locomotion on Compliant legs. Philosophical Transactions of the Royal Society of London- Series B: Biological Sciences *338(1284)*, 189-198.

Biewener, A. A. (1990). Biomechanics of Mammalian terrestrial locomotion. Science *250*, 1097-1103.

Cavagna, G. A., Heglund, N. C., and Taylor, C. R. (1977). Mechanical Work in Terrestrial Locomotion: Two Basic Mechanisms for Minimizing Energy Expenditure. Am. J. Physiol. *233*, R243-R261.

Cavagna, G. A., Saibene, F. P., and Margaria, R. (1964). Mechanical Work in Running. J. Applied Physiology *19*, 249-256.

Cavagna, G. A., Thys, H., and Zamboni, A. (1976). The Sources of External Work in Level Walking and Running. J. Physiol. Lond. *262*, 639-657.

Clarke, T. E., Frederick, E. C., and Cooper, L. B. (1983). Effects of Shoe Cushioning Upon Ground Reaction Forces in Running. Int. J. Sports Med. *4*, 247-251.

Farley, C. T., Blickman, R., Saito, J., and Taylor, C. R. (1991). Hopping Frequency in Humans: A Test of How Springs Set Stride Frequency in Bouncing Gaits. The American Physiological Society, 2127-2132.

Farley, C. T., Glasheen, J., and McMahon, T. A. (1993). Running Springs: Speed and Animal Size. Journal of Experimental Biology *185*, 71-86.

Farley, C. T., and Morgenroth, D. C. (1999). Leg Stiffness Primarily Depends on Ankle Stiffness During Human Hopping. Journal of Biomechanics *32*, 267-273.

Ferris, D. P., and Farley, C. T. (1997). Interaction of Leg Stiffness and Surface Stiffness During Human Hopping. The American Physiological Society, 15-22.

Ferris, D. P., Louie, M., and Farley, C. T. (1998). Running in the Real World: Adjusting Leg Stiffness for Different Surfaces. Proc. R. Soc. Lond. B *265*, 989-994.

He, J., Kram, R., and McMahon, T. A. (1991). Mechanics of Running Under Simulated Low Gravity. The American Physiological Society, 863-870.

Kram, R., and Taylor, C. R. (1990). Energetics of Running: a New Perspective. Nature *346*, 265-267.

McGeer, T. (1990). Passive Bipedal Running. Proc. R. Soc. Lond. *B240*, 107-134.

McMahon, T. A. (1990). Spring-Like Properties of Muscles and Reflexes in Running. In Multiple Muscle Systems: Biomechanics and Movement Organization, J. M. Winters and S. L.-Y. Woo, eds. (Springer-Verlag), pp. 578-590.

McMahon, T. A., and Cheng, G. C. (1990). The Mechanics of Running: How does Stiffness Couple with Speed? Journal of Biomechanics *23*, 65-78.

McMahon, T. A., and Greene, P. R. (1979). The Influence of Track Compliance on Running. Journal of Biomechanics *12*, 893-904.

McMahon, T. A., Valiant, G., and Frederick, E. C. (1987). Groucho Running. J. Appl. Physiol. *62*, 2326-2337.

Nigg, B. M., Bahlsen, H. A., Luethi, S. M., and Stokes, S. (1987). The Influence of Running Velocity and Midsole Hardness on External Impact Forces in Heel-Toe Running. J. Biomech *20*, 951-959.

Taylor, R. C. (1992). Cost of Running Springs. In Physiological Adaptions in Vertebrates: Respiration, Circulation, and Metabolism, S. C. Wood, R. E. Weber, A. R. Hargens and R. W. Millard, eds. (New York: Marcel Dekker, Inc.), pp. 55-65.

Chapter 2
Experiment on Humans Running on Surfaces of Different Compliance

2.1 Introduction

The leg of a running animal can be simplified as a mass-spring system having a point mass, equal to the mass of the animal, located at the hip and a single linear spring as the leg. This representation has described the mechanics of a running leg under different running scenarios remarkable well (Alexander, 1992; Farley et al., 1991; Farley et al., 1993; Farley and Morgenroth, 1999; Ferris and Farley, 1997; Ferris et al., 1998; He et al., 1991; McGeer, 1990; McMahon and Cheng, 1990; McMahon, 1990). Utilizing an actual leg spring has also been shown as an essential means by which humans minimize metabolic cost while running (Alexander, 1988; Alexander, 1992; Cavagna et al., 1964; Cavagna et al., 1976; Cavagna et al., 1977). In this paper, we look at how the leg spring is affected both energetically and mechanically when running on surfaces of different compliance (Figure 2.1).

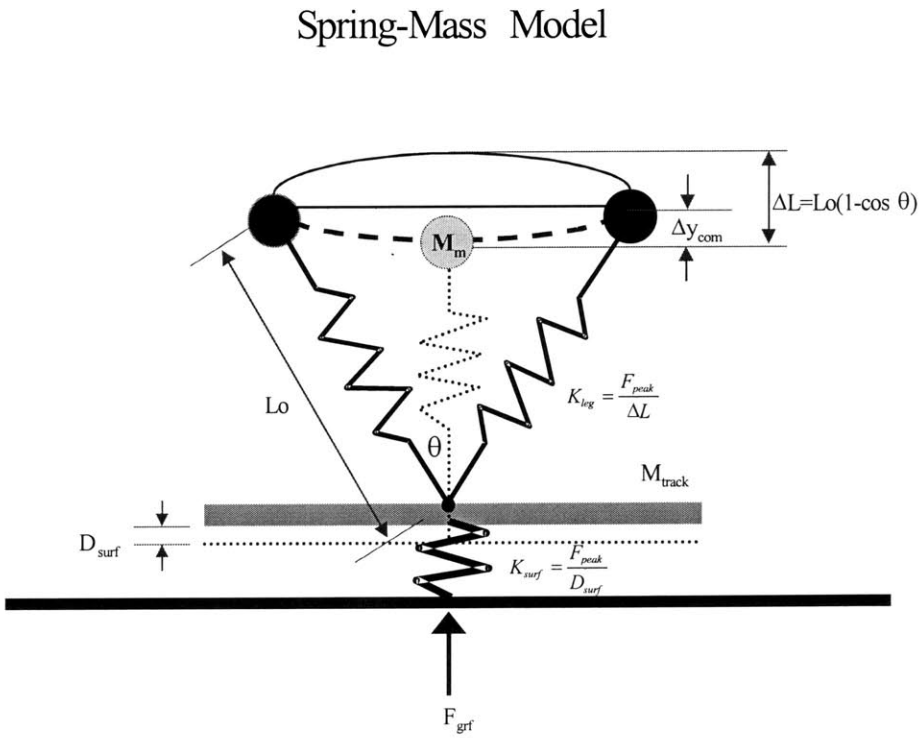

Figure 2.1: A spring-mass model representation of a runner's leg in contact with the ground

McMahon and Greene were the first to study the effects of changing surface compliance on running biomechanics (1979). They discovered a range of compliant surfaces where a runner's performance was enhanced by decreasing foot ground contact time, decreasing the initial spike in peak ground reaction force, and lengthening stride length. Tracks within this enhanced performance range have been built at Harvard University, Yale University, and Madison Square Garden, and have resulted in better running performance by decreasing times by 2-3% and injuries by 50%. Despite the success of these tracks, the reasons behind the performance enhancement are not clearly understood.

McMahon and Cheng described the leg spring as having two stiffnesses: K_{leg} and K_{vert}. K_{leg} is the actual leg stiffness describing the integrated parts of the leg's musculoskeletal system, and K_{vert} is the effective vertical stiffness describing the system's center of mass at mid step (McMahon et al., 1987; McMahon and Cheng, 1990). K_{vert} can be calculated from the ratio of peak vertical ground reaction force (F_{peak}) to the vertical displacement of the center of mass (Δy_{com}):

$$K_{vert} = \frac{F_{peak}}{\Delta y_{com}}. \tag{2.1}$$

Farley et al determined that for a given ground stiffness, K_{leg} changes little with speed (1993). However, later experiments showed that K_{leg} changes when animals run on surfaces of different compliance (Ferris and Farley, 1997; Ferris et al., 1998). Leg stiffness adjustments are due to changes in ankle joint stiffness and to changes in leg posture (Farley et al., 1998). All modeling efforts and experiments have shown that a runner's center of mass deflections remain constant, independent of surface stiffness (K_{surf}), and that this may be a general principle of running (Ferris and Farley, 1997; McMahon and Greene, 1979).

The goal of this thesis is to extend these results by reexamining running on surfaces with a compliance range of 75kN/m to 945 kN/m. Within this ground stiffness range, the energetic cost of running is measured. We hypothesize that the metabolic cost of running decreases when running on the compliant surfaces within the range of the tuned track, and that runners will adapt to these surfaces without altering their overall running dynamics.

2.2 Materials and Methods

2.2.1 Experimental Track Design

In order to test our hypothesis, we built a track with an adjustable stiffness. Since the experiments were conducted on a treadmill, the track surface was limited to platforms that would fit within the size limitations of

the treadmill. We used a treadmill fitted with an AMTI force plate and accessible to a Douglas Bag Oxygen Analyzer setup.

We tested five surface compliances based on ranges found in the literature (Farley et al., 1998; Ferris and Farley, 1997; Ferris et al., 1998; McMahon and Greene, 1979). The McMahon and Greene "tuned track" stiffness (1/compliance) range is between 50kN/m and 100 kN/m (1979). Due to size limitations of the existing treadmill and earlier work done by Farley et al (1998; in press), we designed our variable track surface to go from within the middle of this range: 75.4 kN/m to stiffnesses of 97.5, 216.8, 454.2, and 945.7 kN/m. The indoor track at Harvard University has a surface stiffness of roughly 190 kN/m allowing for a 9mm deflection for an average 75-kg runner (assuming a runner exerts roughly 2.3 x body weight at mid stance). For a similar runner, our track would result in 22.4, 17.4, 7.8, 3.7, and 1.8 mm deflections (D_{surf}), respectively according to the following equation:

$$D_{surf} = \frac{2.3 \cdot W_b}{K_{surf}}. \tag{2.2}$$

The platform design is shown in Figure 2.2. Garrolite (G-10) was chosen as the material for the track platforms because it met all of the design criteria described below and could easily be machined (Current Inc. East Haven, CT). The design consisted of two G-10 planks (1.22 m x 0.254m x 0.0143 m) rigidly supported in the front and simply supported in the rear by 0.016 m thick acrylic. By moving in the existing treadmill rollers, enough slack was provided to fit the platforms under the belt (cut away in the picture to reveal platforms) directly on top of the force plate. Rollers were added to the existing treadmill to reroute the treadmill belt over the platforms, and a frame was built (not shown) to hold the platform in place on top of the force plate during testing. The rear support was movable so that by simply bringing it in closer to or farther away from the front support, the stiffness of the running surface was increased or decreased, respectively.

The design of the platforms was based on simply supported, two-point bending beam theory. Pilot studies showed that this configuration would work well within the size limitations of the treadmill (0.102 m maximum height over the 1.22 m long by 0.457 m wide force plate). Materials and dimensions were chosen based on the maximum deflection (Y_{max}) of the center of the beam according to the factor of safety (FS) associated with the loads that would be applied in running (F) or,

$$Y_{\max} = \frac{-FL^3}{48EI} \tag{2.3}$$

$$FS = \frac{\sigma_u}{\sigma_{\max}}, \tag{2.4}$$

where L is the length of the beam, E is Young Modulus, I is the moment of inertia, σ_u is the ultimate stress of the material, and σ_{max} is the maximum stress of the material.

a) Track Platform Set-Up

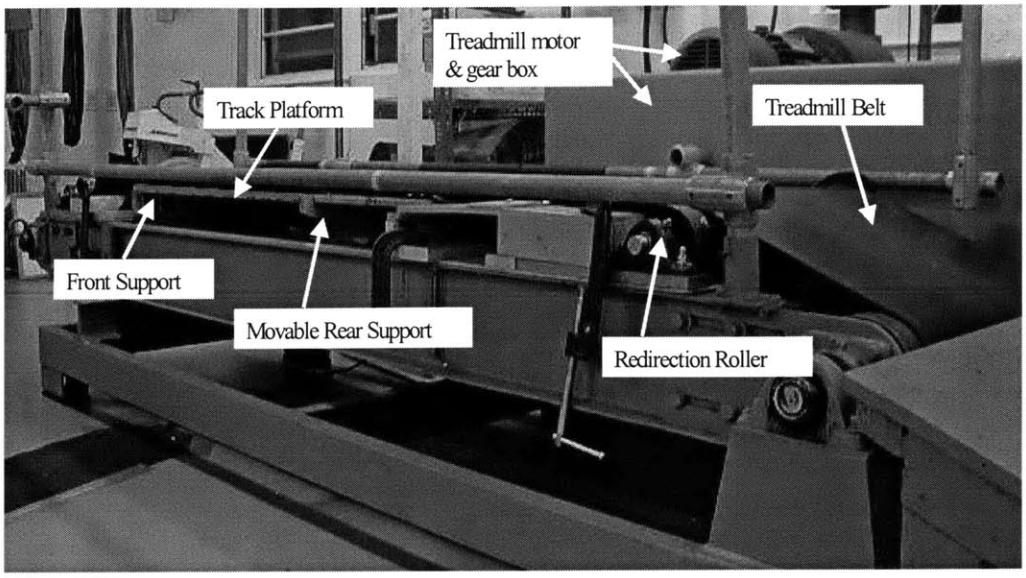

b) Experimental Track

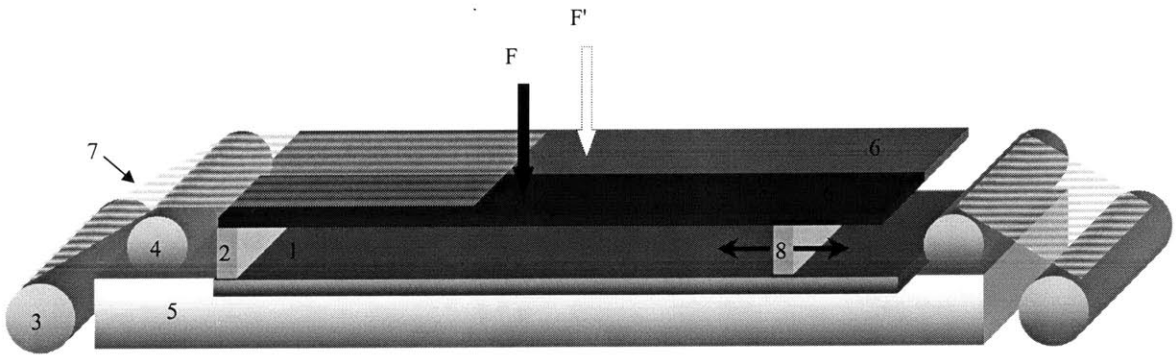

1. Force Plate
2. Front Support
3. Treadmill Roller
4. Redirection Roller
5. Treadmill Base
6. Compliant Running Platform
7. Treadmill Belt
8. Movable Rear Support

Figure 2.2: a) Digital photo of experimental set-up, and b) Drawing of track design

Another design criterion was that the track mass needed to be small enough so that the inertial forces due to the movement of the track would be negligible compared to the forces exerted by the runner's leg. Through modeling the leg and track surface as a two-mass and two-spring system we found that the effective mass of the track had to be less than 12 kg (or 17% of the mass of the runner) (see Chapter 3).

Once installed, the stiffness of the platforms (K_{surf}) was calibrated by statically applying loads to a person and measuring force (F_{peak}, from the force plate) and deflection (D_{surf}, from an LVDT cable extender ±0.25%, Celesco Transducer Products, CA).

$$K_{surf} = \frac{F_{peak}}{D_{surf}} \tag{2.5}$$

Calculating the effective mass of the platforms provided the inertial effects of the track platforms on the force plate. The effective mass of the track (M_{track}) was estimated by finding the damped frequency (ω_d) of the track inserts. The damped frequency was measured by striking the platforms and plotting the displacement verses time for the free vibration of the track surface (Farley et al., 1998). The LVDT cable extender was placed at the center edge of each stiffness configuration, and the platforms were resting on top of the AMTI force plate under the treadmill belt. The damped frequency was computed from the period of vibration (T_d) or,

$$\omega_d = \frac{2\pi}{T_d}. \tag{2.6}$$

The damping ratio of the track surface was also calculated and found to be negligible ($\xi \approx 0.07$). Hence, the effective mass of the track was estimated from the track stiffness (K_{surf}) and the damped frequency, or

$$M_{track} \approx \frac{K_{surf}}{\omega_d^2}. \tag{2.7}$$

The effective mass of the track was then used together with the second derivative of the displacement curves (to obtain acceleration) to estimate the inertial force ($F_{inertial}$) of the track platforms using;

$$F_{inertial} = M_{track} \frac{d^2x}{dt^2}. \tag{2.8}$$

The effective masses (6.88, 8.88, 4.94, 2.65, and 5.39 kg) gave inertial forces of -41.43, -30.41, -10.04, -3.33, and –0.42 N respectively. These forces are less than 2.5% of the peak forces recorded by the force plate and so were ignored.

2.2.2 General Procedures

In this study, eight healthy male subjects (body mass 74.39 ± 7.12 kg; leg length 0.959 ± 0.049 m, mean ± S.D.) ran at 3.7 m/s on a level treadmill fitted with track platforms of five different compliances. All subjects wore the same flat-soled running shoes. Approval was granted from Harvard University's Committee on the use of Human Subjects in Research, and subjects provided signed informed consent. Subjects ran for 5 minutes on each of the compliant track platforms in a mirrored fashion (running on stiffest to softest and then softest to stiffest). Beaded strings hung from the ceiling to give the runner a tactile sign as to where he needed to run so that his mid step corresponded with the center of the track platform. Video was also used to ensure that the runner was centered and not stepping on both sides of the track simultaneously. We recorded ground reaction force (1000 Hz) using a force plate (model OR6-5-1, Advanced Medical Technology, Newton, MA), kinematic data (60 Hz) using an infrared motion analysis system (MacReflex by Qualysis, CA), and oxygen consumption data using a Douglas Bag Analyzer setup (CO2 and O2 analyzers (CD-3A, S-3A), CO2 sensor (P-61B), and Flow Controller (R-2), Ametek, Pittsburg, PA) (Figure 2-3). Force plate and kinematic data were taken simultaneously, and oxygen consumption data were taken after 3 minutes of running so that the subject was at a steady state. Subjects participated in two separate trials so that they ran on each complaint surface four times. Averages were taken on each day and then averaged together for all variables measured.

2.2.3 Force Plate Measurements

Several parameters of interest can be calculated from the force plate data (Kram and Powell, 1989). These parameters can then be indirectly used to calculate the mass-spring characteristics of the runner's leg. LabView (version 4.0.1) was used to acquire the force plate data and output all of the parameters of interest. The force plate was calibrated also using this software by applying known loads to the plate several times and recording the change in voltage on the readout.

Due to the noise from the treadmill belt, motor, and track, we filtered the force data using a lowpass, third order, Butterworth, double reverse filter. The smoothed curve for the ground reaction force was used for analysis. The peak force (F_{peak}) is the force at mid-step and was taken to be the maximum value of this curve. The duration of the force provided us with the ground contact time (t_c) as well as total stride (right foot to right foot) time ($t_c + t_a = dur_{tot}$) that were then used to calculate the stride frequency (freq) and step length (Sl) (right foot to left foot),

$$freq = \frac{Hz}{dur_{tot}}, \tag{2.9}$$

$$Sl = t_c u_x . \tag{2.10}$$

Figure 2.3: Experimental Set-Up

Side View of Experimental Set-Up

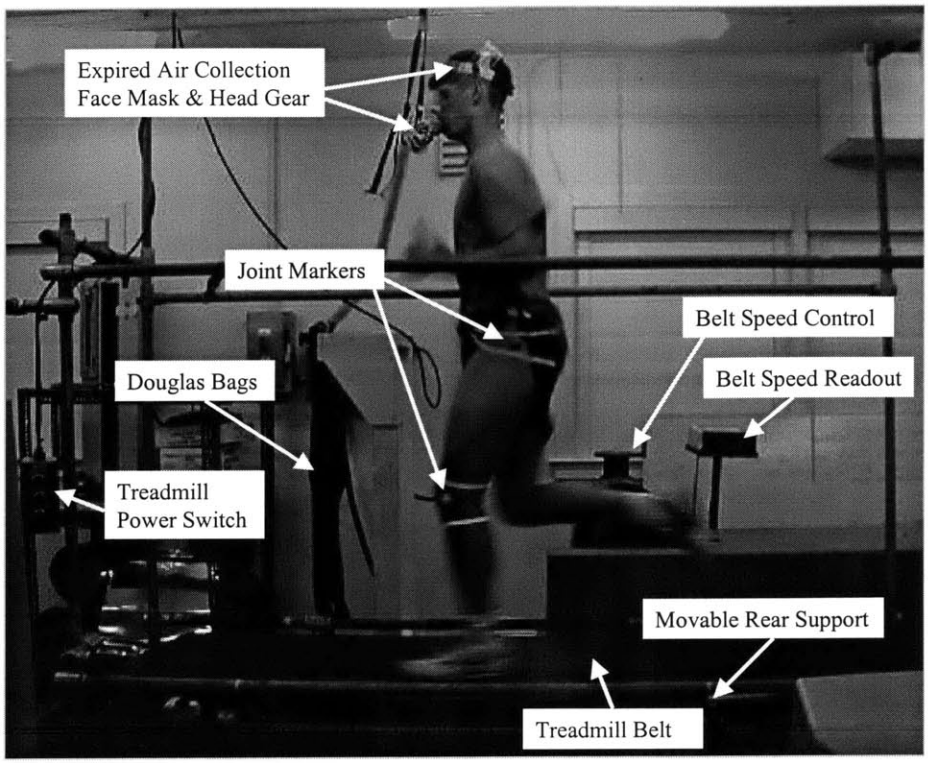

Front View of Experimental Set-Up

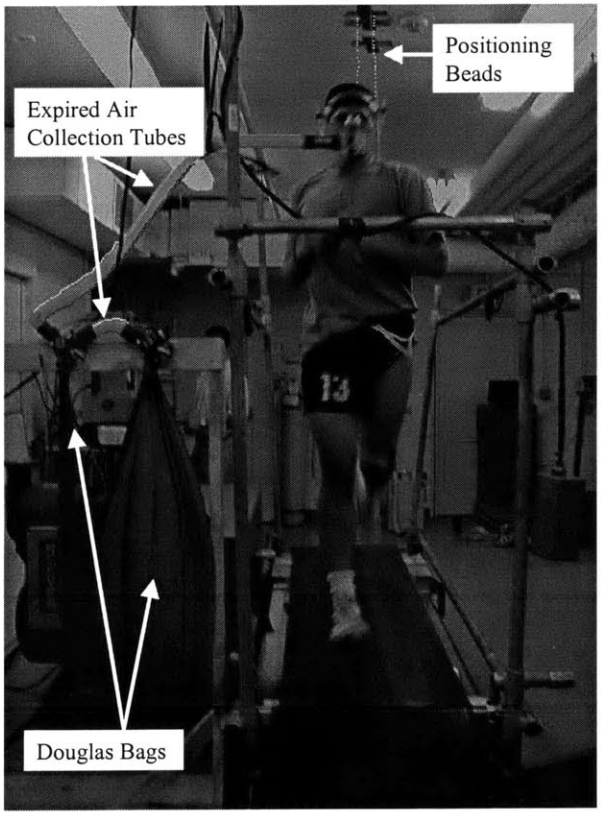

With the additional input of the runner's leg length (L_o) measured from the runner's greater trochanter to the floor while standing straight legged, we calculated half the angle swept by the runner's leg during ground contact (θ) from,

$$\theta = \sin^{-1}(\frac{Sl}{2L_o}). \tag{2.11}$$

Since the ground reaction force is equal to the runner's mass times his acceleration, we were able to calculate the displacement of the center of mass of the runner (Δy_{com}) by twice integrating the vertical acceleration of the center of mass over time (Cavagna, 1975).

On compliant surfaces, the runner's vertical center of mass displacement includes the displacement of the surface (D_{surf}). The surface displacement was simply calculated by using the calibrated values obtained for K_{surf} and the forces form the force plate (Equation 2.5, Figure 2.4).

Mid-Step Track Deflection for 76 kN/m Track Compliance

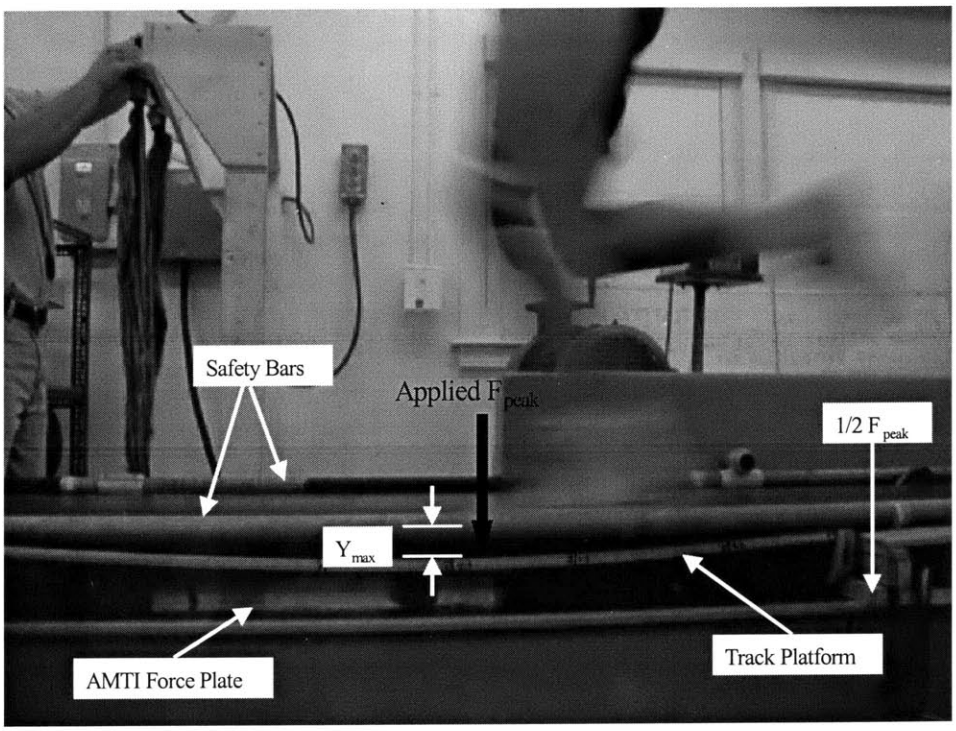

Figure 2.4: Mid-Step Track Deflection

To obtain the relative displacement of the runner with respect to the displacement of the surface, Δy_{rel}, we subtracted the surface displacement from the total center of mass displacement:

$$\Delta y_{rel} = \Delta y_{com} - D_{surf}. \tag{2.12}$$

All of the above variables were then used to calculate the mass-spring characteristics of the runner's leg. The maximum compression of the leg spring (ΔL) was calculated by using the runners leg length (L_o) half the angle swept by the leg during ground contact (θ), and the relative displacement of the runner with respect to the compliant surface (Ferris et al., 1998; McMahon, 1990).

$$\Delta L = \Delta y_{rel} + L_o(1 - \cos\theta) \tag{2.13}$$

Since the peak ground reaction force, F_{peak}, occurs at the same time that the center of mass is the lowest, the stiffness of the leg spring (K_{leg}) was calculated using the ratio of peak ground reaction force to maximum leg compression (Farley and Gonzalez, 1996; He et al., 1991; McMahon, 1990).

$$K_{leg} = \frac{F_{peak}}{\Delta L} \tag{2.14}$$

Similarly, the effective vertical spring stiffness was calculated using the peak force and the total displacement of the center of mass of the system (Equation 2.1).

The total displacement is used in calculating K_{vert} rather than the relative displacement of the runner alone, because on compliant surfaces K_{vert} is affected by the displacement of the surface (Ferris et al., 1998). If the relative displacement was used, there is a possibility that the vertical stiffness, as well as the ground contact time would go negative, and this is not a sensible representation of either variable.

2.2.4 Kinematic Measurements

In order to obtain information on the posture of the limb in contact with the ground, we used an infrared camera system to follow markers that were specifically placed on the subjects. Markers were positioned on the greater trochanter, the lateral epicondyle of the femur, and the lateral malleolus, so that the angle that the lower leg made with the upper leg (knee angle) could be measured. We hypothesized that the leg would be straighter (have a knee angle closer to 180°) at mid step when running on the more compliant surfaces. It was thought that having a straighter limb would contribute to both the increased leg stiffness, and the decreased metabolic energy (Farley et al., 1998). A straighter limb would decrease joint flexion of the leg and therefore increase mechanical

advantage (defined as the ratio of muscle force to ground reaction force) by decreasing joint muscle torques (Biewener, 1989; Ferris and Farley, 1997).

Kinematic data were collected at the same time that force plate data were collected. The data were analyzed using the Maxdos software from MacReflex (Qualysis, CA). These data were then used in a Matlab (version 4.0) program written to calculate the knee angle at mid step (Appendix A). The program took all of the data taken over the 10-second collection period and located the minimum point of the greater trochanter marker. This was assumed to be an estimate of the runner's center of mass, and therefore the point of mid step where force application reached its peak (Farley and Gonzalez, 1996; He et al., 1991; McMahon, 1990). This assumption was confirmed by synchronizing the force plate and kinematic data of one subject using an infrared LED. The frame number of the minimum point was used to locate the position of the other markers at the same instant and the average knee angle was calculated.

The markers were also used to obtain the fluctuations in vertical and horizontal velocity for energy calculations. A curve was fitted to the hip marker's x and y position data using a Matlab program (Appendix B). The derivative of these curves provided the velocity over time in the x and y direction respectively. The change in velocity over ground contact was then taken from the curves.

2.2.5 Measuring Metabolic Cost

To quantify the energetics of human running, we used a Douglas Bag Oxygen Analyzer setup to measure the percent of carbon dioxide (%CO2) and oxygen (%O2) in the runner's expired air. The runners ran aerobically for 3 minutes in order to achieve a steady state. After the third minute, we collected the expired air for 2 minutes using two Douglas bags (1 per minute), a mouthpiece, and a nose clip which were attached to the runner via a special headpiece equipped with a one-way valve. The rate of oxygen consumption (VO2 ml/kg min) was then calculated using the volume of the expired air (V, from a gas volume meter, Parkenson, Cowan), room and vapor pressure corrections (P) body weight (W_b) and the percent CO2 and O2 values.

$$V_{tot} = \left[\left(V_f - V_i + \left(flow\_rate * t_{sample} \right) \right) \left(1 - \frac{t_{collection} - 60s}{t_{collection}} \right) \right] \left[\left(\frac{P_{room} - P_{vapor}}{P_{room}} \right) \left(\frac{273K}{T_{gas}} \right) \right] \quad (2.15)$$

$$\dot{V}O2 = \frac{10(V_{tot}(100 - \%O2 - \%CO2)(0.265) - \%O2)}{W_b} \quad (2.16)$$

$$\dot{V}CO2 = \frac{V_{tot}}{100} \left(\frac{1}{\%CO2} \right) \quad (2.17)$$

We converted the rate of oxygen consumption into energy consumption using an energy equivalent of 20.1 J/ml O2 (Roberts et al., 1998). The cost of transport (COT, the amount of energy needed to move a unit weight a unit distance, J/Nm) was then determined.

$$COT = \dot{V}O2\left(20.1\frac{J}{mlO2}\right)\left(\frac{1}{60s}\right)\left(\frac{1}{9.81\frac{m}{s^2}}\right)\left(\frac{1}{u_x}\right) \tag{2.18}$$

The analyzer was calibrated before each run by pumping several balloons of known gas mixture (16.23% O2 and 4.00% CO2 medical gas mixture, AGA Gas Co, Billrica, MA) through the analyzers.

2.2.6 Statistical Analysis

To determine the statistical significance of each of the measured variables over surface stiffness, we used a one-way ANOVA with repeated measures. Using the 5 levels of K_{surf} as the independent variable, and speed, mass, leg length, and marathon runner as covariates, all the data were run through two statistical software packages to determine the p-values and relationships between the means (BMDP, and STATA). Significance ($p<0.05$) was found for almost all variables despite nearly horizontal linear graphs and large standard deviations. This was most likely due to the high power of our study, having an n=40. By looking at the means over each surface and determining that the largest percent difference between any two points was ≤ 5%, we determined that this significance did not prove to be relevant over the variables that appeared to be constant. Excel was then used to plot the calculated means and standard deviations of all variables. A linear regression on the means over the logarithm of K_{surf} using STATA was used to check the fit (all $R^2 \geq 0.83$) and Excel's calculated equation of the curve.

2.3 Results

The track platforms and experimental setup served quite well to provide the desired stiffness range. The runners maintained similar running dynamics on all surfaces, despite the 12-fold change in surface stiffness. This similarity can been seen from the constancy of the ground contact time, step length, sweep angle, stride frequency, duty factor, and peak vertical force (Figures 2.5, 2.6).

The runners also achieved a total constant stiffness for the combination of their leg and the track platform in series ($K_{tot,L}$).

$$\frac{1}{K_{tot,L}} = \frac{1}{K_{leg}} + \frac{1}{K_{surf}} = CONSTANT \tag{2.19}$$

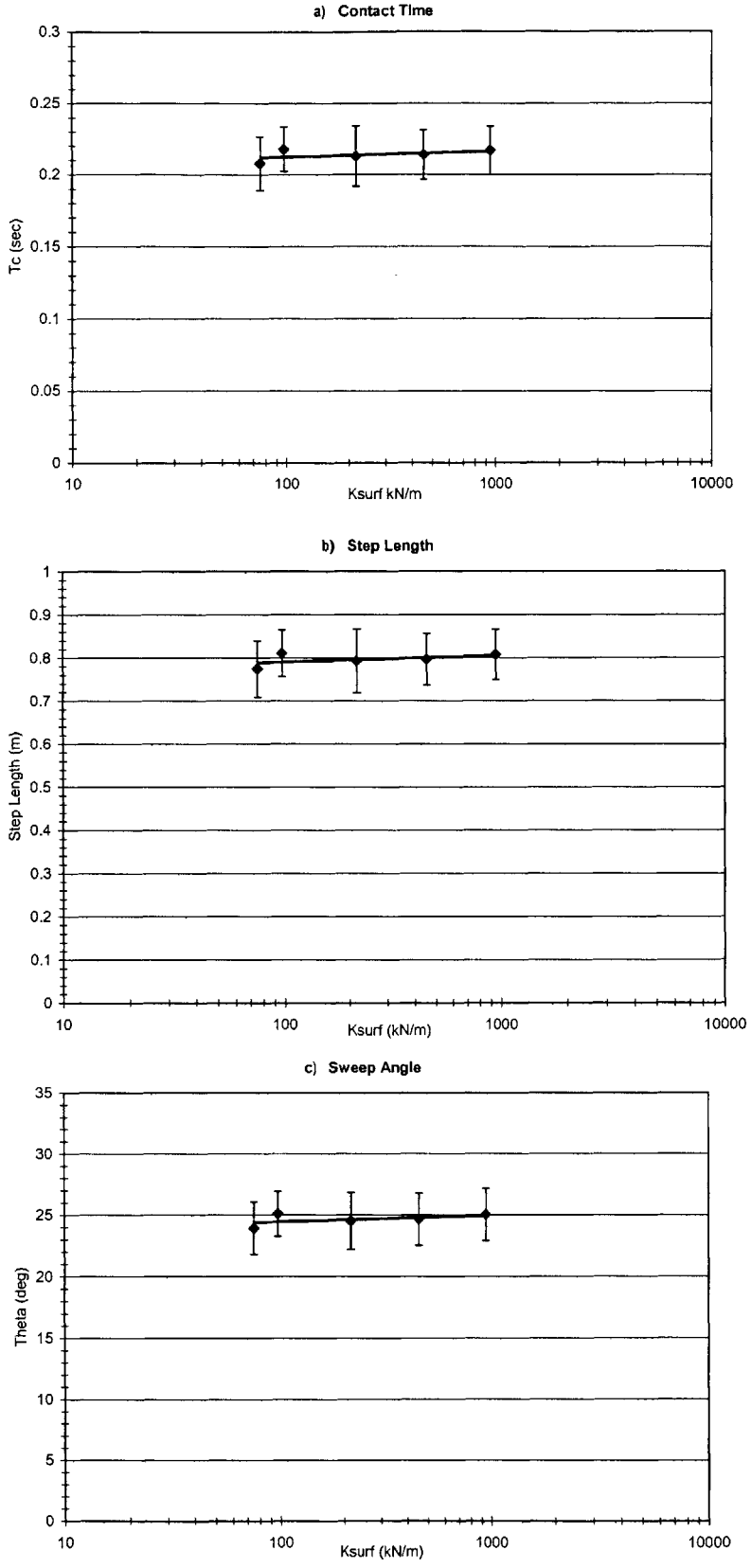

Figure 2.5: a) Ground contact time ±s.d., b) Step length ±s.d., and c) Sweep angle ±s.d.

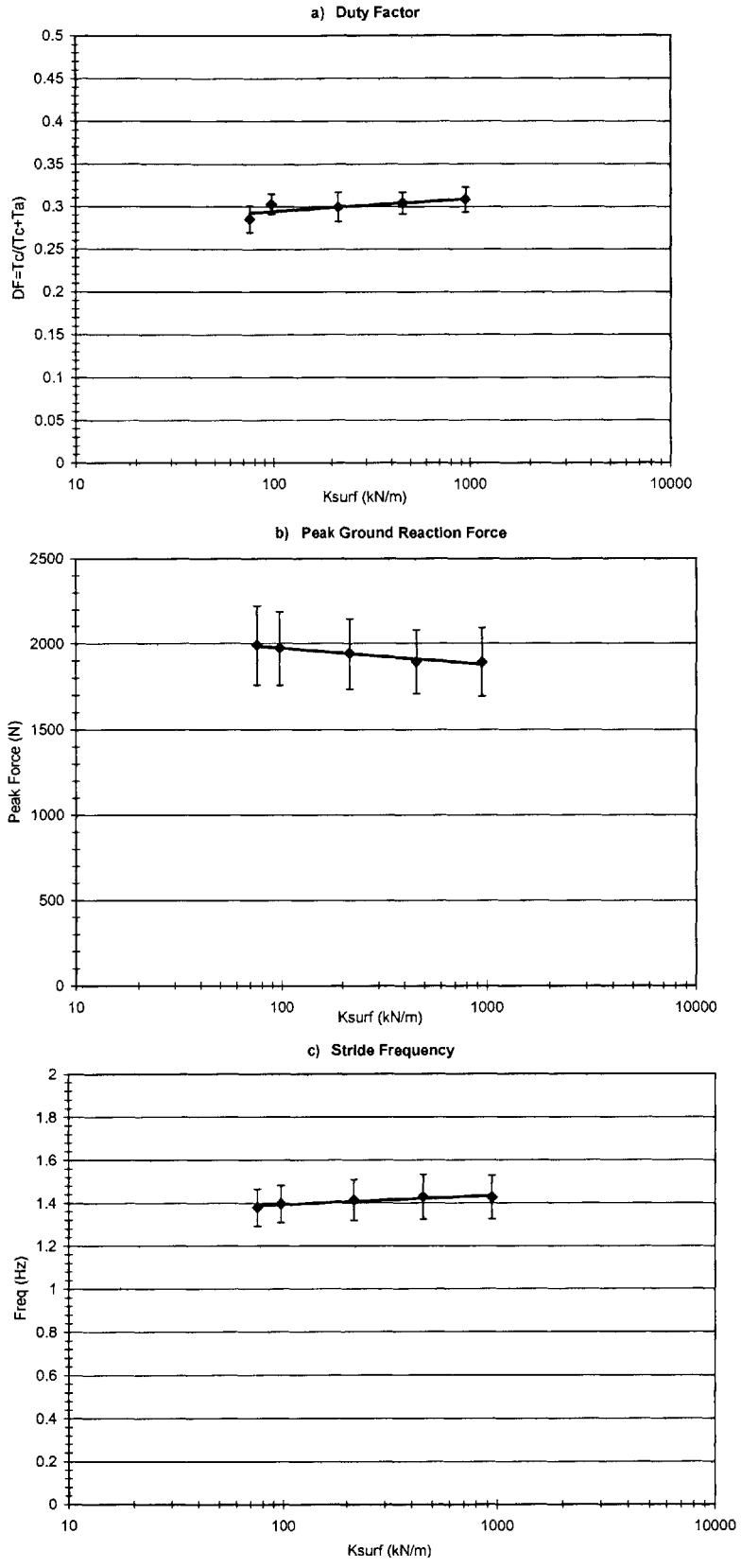

Figure 2.6: a) Duty Factor ±s.d., b) Peak ground reaction Force ±s.d., and c) Stride frequency ±s.d.

Therefore, as the surface stiffness decreased, the runner's leg stiffness increased by 29% (p=0.000) to maintain an overall constant stiffness (Figure 2.7 a, b). The increase in the runner's leg stiffness resulted from a decrease in the amount that their leg spring compressed (Figure 2.7 c).

The overall vertical stiffness (K_{totV}) was not constant, however. Similar to recent studies, the runners maintained approximately a constant effective vertical stiffness over all surfaces (Ferris et al., 1998). Therefore when this constant effective vertical stiffness is added to the changing stiffness of the surfaces, the overall vertical stiffness of the system is not constant (Figure 2.8 a, b).

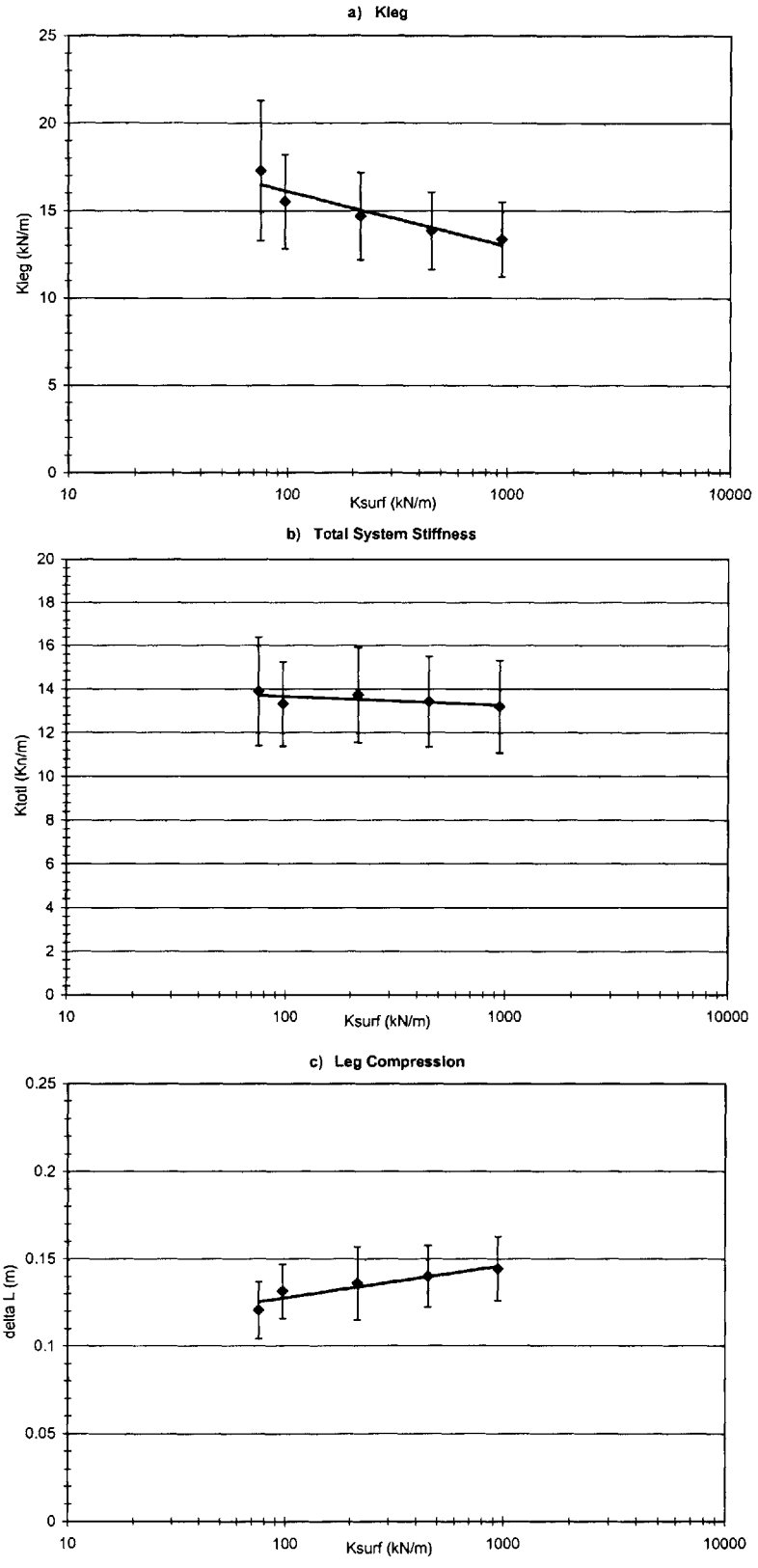

Figure 2.7: a) Leg spring stiffness ±s.d., b) Total system stiffness due to the leg spring ±s.d., and c) Leg compression ±s.d.

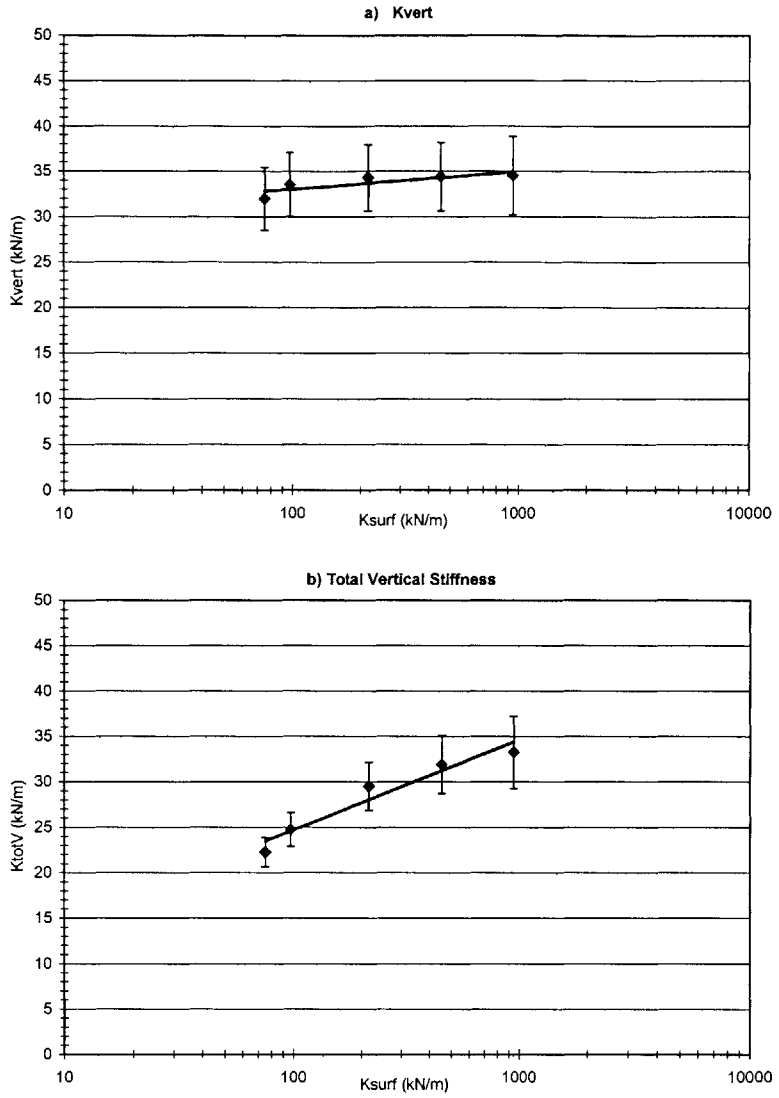

Figure 2.8: a) Effective vertical spring stiffness ±s.d., and b) total vertical stiffness of system ±s.d.

Despite rather large variability at each surface stiffness, a 15% decrease (p=0.00) in the vertical displacement of the runner's center of mass with K_{surf} was observed (Figure 2.9 a). The relative displacement of the runner, however, does indeed change, and this change is quite clear (p=0.00) (Figure 2.9 c). Since the surface displacement increases and the relative displacement decreases as K_{surf} decreases, it is possible to consider these two variables canceling each other out and therefore the vertical displacement of the center of mass would not change over the different surfaces (Figure 2.9). Assuming that the runner's center of mass displacement does not significantly change over surfaces is in agreement with previous studies (Farley et al., 1998; Ferris et al., in press; McMahon and Greene, 1979).

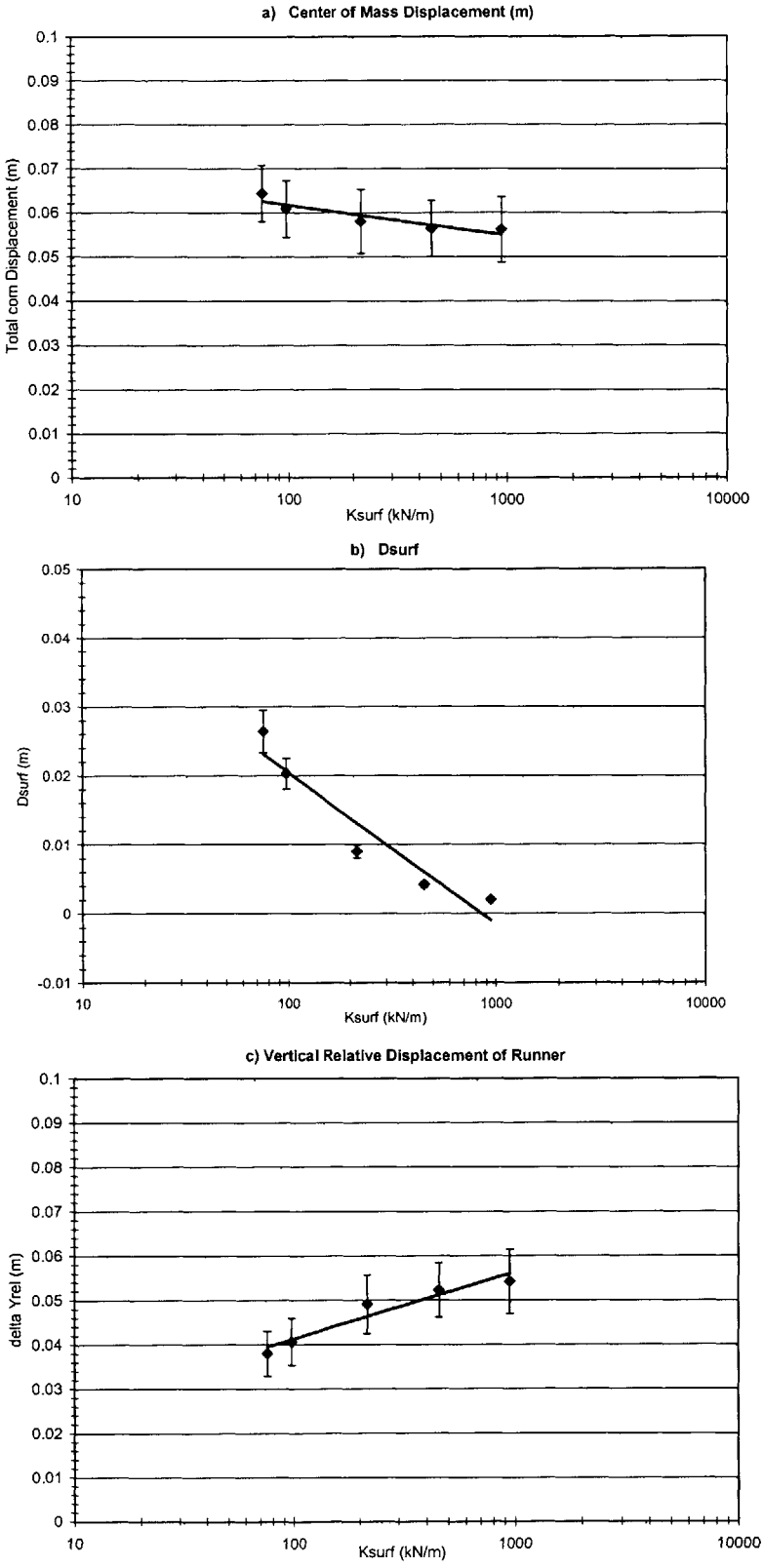

Figure 2.9: a) Total displacement of the runner's center of mass, b) Surface displacement, and c) Relative displacement of the runner's center of mass with respect to the surface displacement ±s.d.

We also found that the runner's cost of transport decreased by 12% as surface stiffness decreased. Kram and Taylor showed that the cost of transport could be calculated from velocity, ground contact time, and a cost coefficient that relates the cost of muscle force generation to ground contact force (1990). Since contact time (t_c) and forward speed (u_x) were constant over all surfaces, this means that the cost coefficient (C_o) also decreased with decreasing K_{surf} (Figure 2.10 a, b).

$$COT = \frac{C_o}{u_x t_c} \tag{2.20}$$

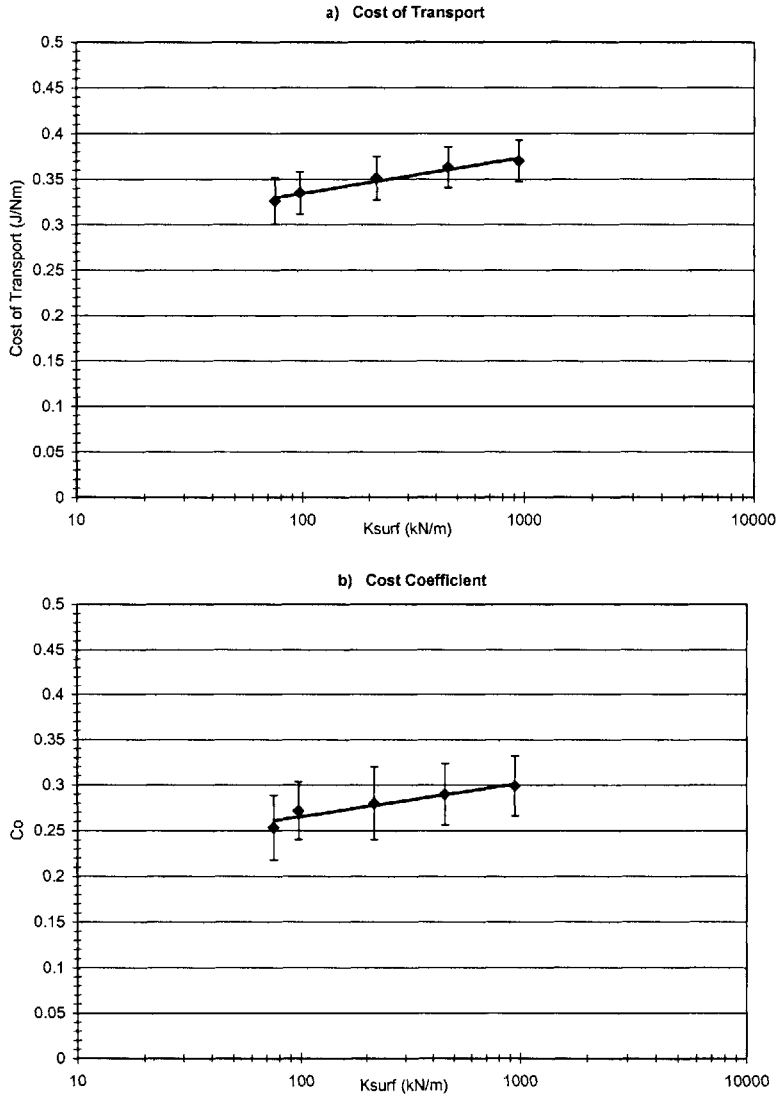

Figure 2.10: a) Cost of Transport, and b) Cost coefficient ±s.d.

Kram and Taylor found that the cost coefficient remains constant over a range of speeds. This result is based on several assumptions. Our data suggests that at least one of these assumptions is violated when running over surfaces of different compliance. It seems likely that the amount of active muscle used to support the runner's body weight is not held constant as was assumed by Kram and Taylor (1990). A constant volume of active muscle would result from a constant mechanical advantage. Again, mechanical advantage is defined as the ratio of muscle force to ground reaction force (Biewener, 1989). Although the mechanical advantage could not be calculated in our experiment, the decrease in cost of transport with contact time and velocity, suggest that limb mechanical advantage changes when running over surfaces of different compliance.

We tried to approximate the mechanical advantage of the leg by looking at limb posture. An accurate measure of mechanical advantage was not possible because the treadmill force plate does not reliably track horizontal forces. We therefore used the kinematic joint data, along with the vertical ground reaction force, to calculate the angle the upper leg made with the lower leg (knee angle) over all surfaces at mid step. Knowing that K_{leg} increased, we assumed that part of this increase could bc due to a straighter leg at mid-step. The results do show a slight straightening of the leg by 2% for running on the more compliant surfaces, and this may be enough to have an effect on mechanical advantage (Figure 2.11a). However, this small change in knee angle was small enough that an estimate of joint torque was not significant (p=0.1123) (Figure 2.11 b).

McMahon and Green had postulated that a reduction in both leg muscle force production and work production might contribute to the enhanced performance they observed on their tuned track (1979). The elastic track itself may partially be the cause of a reduced work output by storing and returning energy to the runner. In fact, the McMahon and Green track stored and returned roughly 9% of the energy required for each step. We calculated the energy return of our track platforms by using the maximum track deflection to derive the potential energy due to the track spring (E_{track}):

$$E_{track} = \frac{1}{2} K_{surf} \max(D_{surf})^2 . \tag{2.21}$$

We also used the experimental data to calculate the total mechanical energy of the center of mass of the runner (E_{com}). The change in this energy from mid step to takeoff is an estimate of the energy required to power a running step. The center of mass of a running person has three energies: forward kinetic energy (E_{kf}), vertical kinetic energy (E_{kv}), and gravitational potential energy (E_p). These were computed using the runner's mass (M_m), change in speed (Δu_x and Δv_y), gravitational acceleration, (g), and change in the relative displacement of the runner (Δy_{rel}):

$$E_{kf} = \frac{1}{2} M_m (\Delta u_x)^2 \tag{2.22}$$

$$E_p = M_m g \Delta y_{rel} \tag{2.23}$$

$$E_{kv} = \frac{1}{2} M_m (\Delta v_y)^2 . \tag{2.24}$$

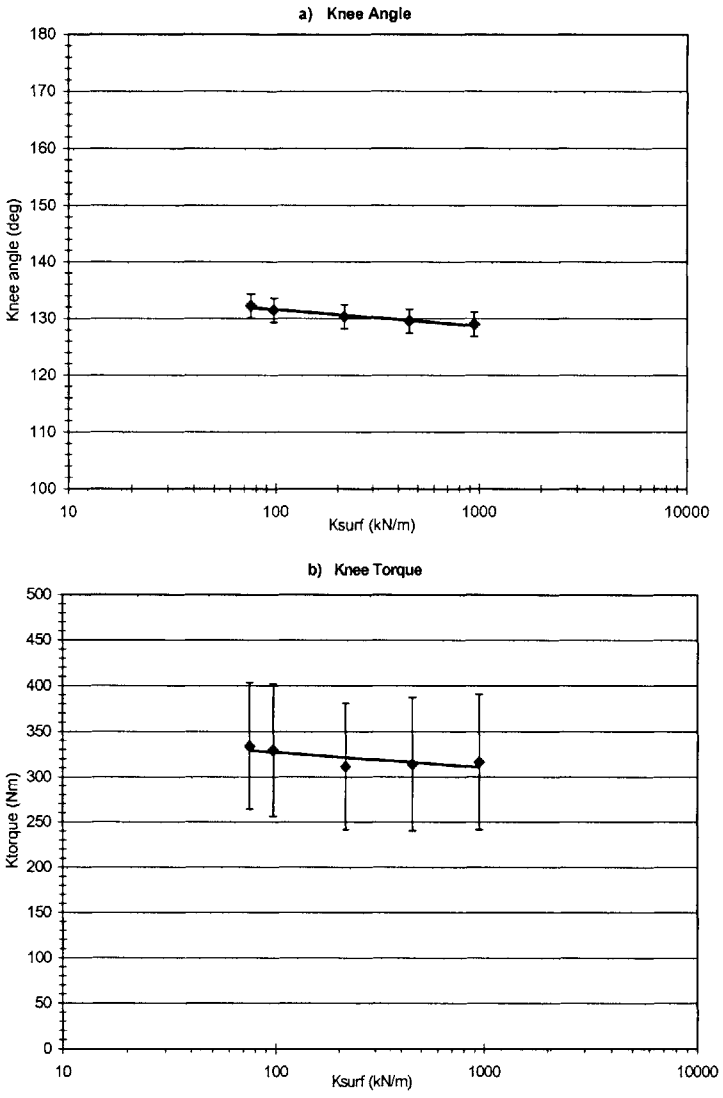

Figure 2.11: a) Knee angle, and b) Knee torque ±s.d.

From these calculations, the E_{com} decreases and the E_{track} increases with decreasing surface stiffness (Figure 2.12). Comparing E_{com} to E_{track} we found that the track did perhaps return a large fraction of the energy required to power the leg during ground contact time. In fact a 27% return was observed at the lowest stiffness.

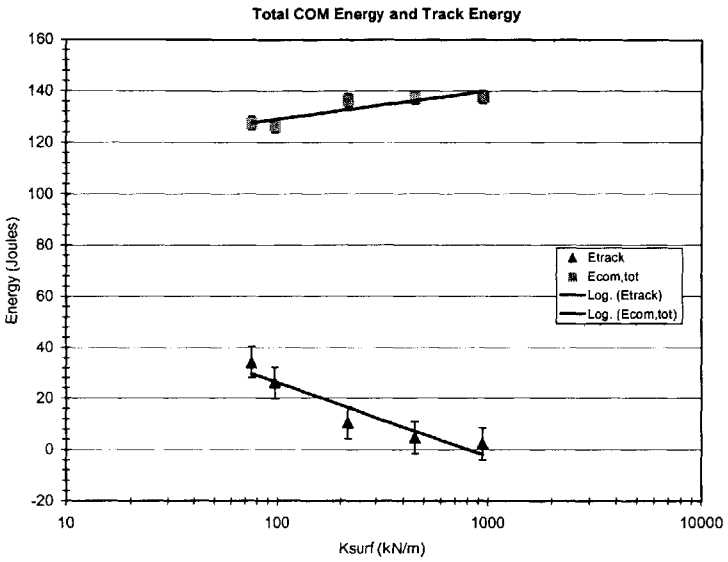

Figure 2.12: The runner's center of mass energy compared to the energy return from the track ±s.e.

2.4 Discussion

McMahon and Greene were the first to look at the effects of surface compliance on the mechanics of human running (1979). More recently, Ferris and Farley studied surface effects on the hopping and running leg spring and proposed ideas on the underlying mechanism of leg stiffness adjustment (Farley et al., 1998; Farley and Morgenroth, 1999; Ferris and Farley, 1997; Ferris et al., 1998). These studies provide insight into the mechanics of human running, but do not specifically address running energetics.

In this study, we relate both the energetic and mechanical effects of running on surfaces of different compliance in order to gain additional insight into human running. Our findings support Farley et al's findings and suggest that human runners do indeed alter their leg spring stiffness to compensate for changes in surface compliance. The mechanism for this change is not clear from this study, but is likely due to a combination of an increase in joint stiffness and limb posture (Farley and Morgenroth, 1999). We also found that human runners appear to alter their leg stiffness in an effort to lower the cost of running over these surfaces. Compared to running on a hard surface, the runner's cost of transport was reduced by 12% when running on surfaces that were 12 times more compliant. This suggests that there is both a mechanical and energetic benefit to running on a "tuned track".

What accounts for the decreased metabolic energy when running on more compliant surfaces? Although the leg is assumed to behave like a linear spring, it does not behave like an ideal spring. If it were ideal, it would be almost completely passive. In other words energy would only need to be added to the system initially to get the leg going, and then the elastic storage and recoil of the spring alone would be enough to power the runner indefinitely. This is obviously not the case. Running consumes metabolic energy because the muscles are active, supporting the weight of the runner and supplying energy to operate the leg spring (Taylor, 1992). A muscle generates its maximal force and consumes the lowest amount of energy when operating isometrically, i.e. at zero velocity (Taylor, 1992). More specifically, the cost of producing force while running can be minimized by operating the active muscle fibers isometrically while using the tendon springs to provide the work needed to move the body forward (Roberts et al., 1997). Roberts et al also found that the tendon energy storage and recoil provided roughly 60% of the work involved in running for the one muscle studied. Since less work is required by the muscles themselves, it is thought that less active muscle volume is needed to support the weight of the runner (Roberts et al., 1997).

In our experiment we did not put strain gauges on the muscles of our human runners so we can not determine to what extent the muscles are shortening. However, we are certain that both the metabolic energy required to power a running step decreases and the energy stored in the track increases on more compliant surfaces (Figures 2.10 a, 2.12). Since the metabolic energy decreases on the more compliant surfaces, the leg musculature (muscle bellies and tendons) must be doing less work from mid step to take off. More detail cannot be determined without knowing the extent of muscle shortening. It is also possible that the decrease in the total mechanical energy of the center of mass may be supported by an increase in the amount of energy that the track is returning to the system. If the system were perfect, it would be possible to have the track return to the runner as much as 27% of the work required to power the running step. However, it is probably not a perfect system, and despite the track storing a large amount of energy, we have no proof that any of the energy is actually returned to the runner.

There is a limit to how much we can reduce the cost of running on compliant surfaces. This study might suggest that the lower the surface compliance, the lower the cost of running. In reality, running on pillows or sand is a lot of work, and running on a soft trampoline is nearly impossible. We only looked at surfaces that were within a specific compliance range that had already demonstrated an enhanced running performance (McMahon and Greene, 1979). It would be useful to extend our results by doing an experiment where the stiffness range goes beyond that of the "ideal" range. We believe that for lower stiffnesses than those studied here, the cost of transport would begin to rise when the leg can no longer accommodate changes in the environment of the running surface. This rise would most likely be partially due to having less stability on these surfaces. Expanding the surface range would allow us to find a true energetic minimum for running. Based on subject feedback, running on the softer to mid-range surfaces were preferred to running on the harder ones. However,

subjects felt that they were beginning to compensate for the deflections of the softer surfaces by shifting their weight from side to side, compared with the harder surfaces that felt more stable. It would also be interesting to test surfaces actually encountered in the real world to see if people are indeed experiencing a metabolic cost reduction when running on them.

Many of the results and ideas presented here are based on the assumption that the running leg behaves as a linear spring. In Chapter 3, a mathematical model of the mass-spring system of the runner and track is presented. The model predicts well how running mechanics change with ground compliance.

2.5 References

Alexander, R. M. (1988). Elastic Mechanisms in Animal Movement (Cambridge UK: Cambered University), pp. 30-50.

Alexander, R. M. (1991). Energy-Saving Mechanisms in Walking and Running. Journal of Experimental Biology *160*, 55-69.

Alexander, R. M. (1992). The Human Machine, R. M. Alexander, ed. (London: Natural History Museum Publications).

Alexander, R. M. (1992). A Model of Bipedal Locomotion on Compliant legs. Philosophical Transactions of the Royal Society of London- Series B: Biological Sciences *338(1284)*, 189-198.

Biewener, A. A. (1990). Biomechanics of Mammalian Terrestrial Locomotion. Science *250*, 1097-1103.

Biewener, A. A. (1989). Scaling Body Support in Mammals: Limb Posture and Muscle Mechanics. Science *245*, 45-48.

Cavagna, G. A. (1975). Force Platforms as Ergometers. Journal of Applied Physiology *39*, 174-179.

Cavagna, G. A., Heglund, N. C., and Taylor, C. R. (1977). Mechanical Work in Terrestrial Locomotion: Two Basic Mechanisms for Minimizing Energy Expenditure. Am. J. Physiol. *233*, R243-R261.

Cavagna, G. A., Saibene, F. P., and Margaria, R. (1964). Mechanical Work in Running. J. Applied Physiology *19*, 249-256.

Cavagna, G. A., Thys, H., and Zamboni, A. (1976). The Sources of External Work in Level Walking and Running. J. Physiol. Lond. *262*, 639-657.

Clarke, T. E., Frederick, E. C., and Cooper, L. B. (1983). Effects of Shoe Cushioning Upon Ground Reaction Forces in Running. Int. J. Sports Med. *4*, 247-251.

Farley, C. T., Blickman, R., Saito, J., and Taylor, C. R. (1991). Hopping Frequency in Humans: A Test of How Springs Set Stride Frequency in Bouncing Gaits. The American Physiological Society, 2127-2132.

Farley, C. T., Glasheen, J., and McMahon, T. A. (1993). Running Springs: Speed and Animal Size. Journal of Experimental Biology *185*, 71-86.

Farley, C. T., and Gonzalez, O. (1996). Leg Stiffness and Stride Frequency in Human Running. Journal of Biomechanics *29*, 181-186.

Farley, C. T., Houdijk, H. H. P., Strien, C. V., and Louie, M. (1998). Mechanism of Leg Stiffness Adjustment for Hopping on Surfaces of Different Stiffnesses. J. Appl. Physiol. *85*, 1044-1055.

Farley, C. T., and Morgenroth, D. C. (1999). Leg Stiffness Primarily Depends on Ankle Stiffness During Human Hopping. Journal of Biomechanics *32*, 267-273.

Ferris, D. P., and Farley, C. T. (1997). Interaction of Leg Stiffness and Surface Stiffness During Human Hopping. The American Physiological Society, 15-22.

Ferris, D. P., Liang, K., and Farley, C. T. (in press). Runners Adjust Leg Stiffness for Their First Step on a New Running Surface. .

Ferris, D. P., Louie, M., and Farley, C. T. (1998). Running in the Real World: Adjusting Leg Stiffness for Different Surfaces. Proc. R. Soc. Lond. B *265*, 989-994.

He, J., Kram, R., and McMahon, T. A. (1991). Mechanics of Running Under Simulated Low Gravity. The American Physiological Society, 863-870.

Kram, R., and Powell, J. (1989). A Treadmill-Mounted Force Platform. J. Appl. Physiol. *67*, 1692-1698.

Kram, R., and Taylor, C. R. (1990). Energetics of Running: a New Perspective. Nature *346*, 265-267.

McGeer, T. (1990). Passive Bipedal Running. Proc. R. Soc. Lond. *B240*, 107-134.

McMahon, T. A. (1990). Spring-Like Properties of Muscles and Reflexes in Running. In Multiple Muscle Systems: Biomechanics and Movement Organization, J. M. Winters and S. L.-Y. Woo, eds. (Springer-Verlag), pp. 578-590.

McMahon, T. A., and Cheng, G. C. (1990). The Mechanics of Running: How does Stiffness Couple with Speed? Journal of Biomechanics *23*, 65-78.

McMahon, T. A., and Greene, P. R. (1979). The Influence of Track Compliance on Running. Journal of Biomechanics *12*, 893-904.

McMahon, T. A., Valiant, G., and Frederick, E. C. (1987). Groucho Running. J. Appl. Physiol. *62*, 2326-2337.

Nigg, B. M., Bahlsen, H. A., Luethi, S. M., and Stokes, S. (1987). The Influence of Running Velocity and Midsole Hardness on External Impact Forces in Heel-Toe Running. J. Biomech *20*, 951-959.

Roberts, T. J., Kram, R., Weyand, P. G., and Taylor, R. (1998). Energetics of Bipedal Running I. Metabolic Cost of Generating Force. The Journal of Experimental Biology *201*, 2745-2751.

Roberts, T. J., Marsh, R. L., Weyand, P. G., and Taylor, C. R. (1997). Muscular Force in Running Turkeys: The Economy of Minimizing Work. Science *275*, 1113-1115.

Taylor, R. C. (1992). Cost of Running Springs. In Physiological Adaptions in Vertebrates: Respiration, Circulation, and Metabolism, S. C. Wood, R. E. Weber, A. R. Hargens and R. W. Millard, eds. (New York: Marcel Dekker, Inc.), pp. 55-65.

Chapter 3

Modeling the Leg Spring on a Compliant Surface

3.1 Introduction

Using computer models to simulate a real situation can be a powerful tool. A human runner is often modeled as a point mass and linear spring system. McMahon and Cheng were among the first to do this (1990) based on earlier findings that the leg has elastic components that store and return energy like a linear spring (Cavagna et al., 1977). Their goal was to develop the simplest possible model of running that was still capable of explaining and predicting known theories about running. Their results supported the assumption that the leg can be represented by a linear spring with constant stiffness when running at different speeds on a hard surface. Another study had shown that a hopping person's leg alters its stiffness to accommodate changes in surface compliance (Ferris and Farley, 1997). Farley et al used a similar mass-spring model to study how a leg's joint stiffness affects the stiffness of the entire leg when hopping on surfaces of different compliance (Farley et al., 1998). Again, they found support for the assumption that the leg behaves as a linear spring, and also that K_{leg} changed on different surfaces primarily because of changes in ankle stiffness.

Computer models take the physics of the experimental situation and use accepted laws and theories to simulate the physical system. Assumptions and hypotheses can be easily tested using models because models are often the simplest representation of the real situation. A deeper understanding of a complex system can be obtained using a simple representation of the general structure of the whole system. Models are also useful predictive tools. By altering the parameter of interest, a model can be used to reproduce experimental data. Once the model is predicting the experimentally known data, it can be used to predict what has yet to be done, or can not be accomplished experimentally. Models are also often used as design tools, allowing the designer to test a material or geometry before actually building the device.

In this thesis, we have developed a model to do all of the above mentioned things. Our model is a representation of a running leg in contact with a compliant surface. Developing the model provided insight into how the system works, and how to best represent it in a simple manner. We used a point mass on top of a linear spring to represent the running leg. The leg spring is then connected to a mass supported by a spring and damper representing the compliant surface. The model helped in designing the track platforms used in the experiment. It also allowed us to test our assumption that the leg behaved as a linear spring while running on compliant surfaces. Finally, we used the model to predict the experimental data (Chapter 2) and to see what would happen to the system if K_{leg} did not change (as was originally assumed in McMahon and Cheng's model (1990) for running at different speeds) to accommodate for changes in surface compliance.

When using models it is important to keep in mind that, although a useful virtual tool, they are not the actual situation and many assumptions still have to be made. Nothing can replace an actual physical situation, but a model is meant to be a learning tool and is used as such here.

3.2 Materials and Methods

3.2.1 *Assumptions and Expectations*

The underlying concept governing the dynamics of the model is that the system behaves in a symmetric manner. For instance, imagine a person on a pogo stick. The pogo stick initially touches down with an unstretched spring at a certain angle and with a certain forward velocity. While remaining in contact with the ground, and pivoting on the point of contact, the spring begins to deflect as the pogo stick moves down and forward. At the peak of this deflection, the person and pogo stick are completely upright, with zero vertical velocity, and the ground reaction force reaches its maximum. At this point the vertical velocity changes and the pogo stick's spring begins to recoil to aid momentum in bringing the person forward and upward until the spring has once again reached its rest length. At this point, the person enters an aerial phase taking off with the same angle, forward velocity magnitude, and vertical velocity magnitude with which they had landed. Adding a vertically moving contact point to this scenario describes our model rather well.

In our model, we assume that the leg can be represented by an undamped, linear spring. The spring attempts to represent the behavior of the entire limb including all of the joints. Therefore the spring is actually a virtual spring that connects the center of mass to the ground contact point. We also assume that the stiffness of this spring (K_{leg}) is constant while in contact with the ground, since K_{leg} is fixed by the initial sweep angle and a level trajectory (McMahon, 1990). The choice of K_{leg} for each compliant surface is critical in maintaining a symmetric and stable model (Ferris et al., in press; McMahon and Greene, 1979). If K_{leg} is too stiff, the leg will take off from the ground too soon causing the runner to lean back off balance. If K_{leg} is too soft, than the body rises too late and the runner's toes would strike the ground. The spring is mounted by a point mass equal to the mass of the runner and roughly located where the runner's center of mass is. The undeflected (rest) length of the leg spring is considered equal to that of the leg length of the runner (L_o). It is assumed that the runner lands with the leg spring at its rest length and takes off when the leg spring is slightly larger than this length. On take off, the leg length is slightly larger than its initial length due to a fully extended knee and a plantar flexed ankle (He et al., 1991).

The model is expected to reproduce the behavior consistent to what is already known about running mechanics. For instance, the vertical velocity and the center of mass' trajectory over time should remain constant over all surfaces (Farley et al., 1998; Ferris et al., in press; McMahon and Cheng, 1990). The mean horizontal velocity should also remain constant over surface compliance.

Finally, the system is considered to follow basic Newtonian dynamics. The track mass is modeled using the effective mass of the track and is restricted to move in the vertical direction only. Therefore, we expect the track mass to have zero initial and final vertical velocities, and to maximally compress its linear spring at mid step. A damper is included to reduce the noise of the oscillating compliant track mass as it deflects.

3.2.2 *Description of the Model*

As described earlier, the model consists of two masses, two springs, and a damper (Figure 3.1). The model only considered the time that the runner's foot is in contact with the ground during a step. Therefore, the leg spring is attached to the track mass at its center of mass, and both it and the track spring maintain a constant stiffness throughout the step. The effective track mass is restricted to move in the vertical direction only. The runner's mass is a point mass located on top of the leg spring. The origin of the system's axes (or true ground) is taken to be the undeflected track (i.e. at the moment of touchdown).

Configuration for Mass-Spring Model

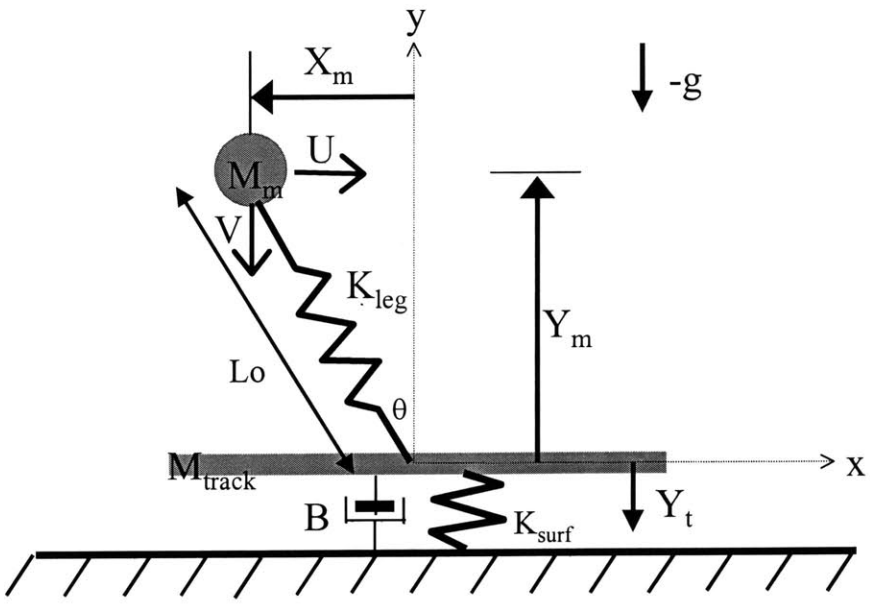

Figure 3.1: Mass-spring model configuration of running leg and compliant surface

Using this configuration we developed free body diagrams so that Newtonian dynamics could be applied in solving the equations of motion for the system (Appendix C). A solution using Langrangian dynamics was also completed to make certain these results were correct.

Agreement was reached using both methods. The three equations of motion that define the system were then formulated into dimensionless variables so that the results of the model were valid for runners of all sizes (Appendix C).

$$\frac{d^2X_m}{dT^2} + K_{LEG}\left[1 - \left((Y_m - Y_t)^2 + X_m^2\right)^{1/2}\right]\sin\theta = 0 \tag{3.1}$$

$$\frac{d^2Y_m}{dT^2} - K_{LEG}\left[1 - \left((Y_m - Y_t)^2 + X_m^2\right)^{1/2}\right]\cos\theta + 1 = 0 \tag{3.2}$$

$$\frac{d^2Y_t}{dT^2} + BW + RK_{LEG}MY_t + K_{LEG}\left[1 - \left((Y_m - Y_t)^2 + X_m^2\right)^{1/2}\right]\cos\theta + 1 = 0 \tag{3.3}$$

A Matlab (version 4.0) program was written to solve these equations of motion given the initial conditions for K_{leg}, position, velocity, mass, leg length, and K_{surf} (Appendix D). The ODE45 numerical solver in Matlab (a Runge-Kutta algorithm) was employed to integrate the equations of motion forward in dimensionless time. The solutions of the equations were then used to output the same variables calculated in the experiment: K_{vert}, K_{leg}, F_{peak}, Sl, t_c, ΔL, Δy_{rel}, Δy_{com}, freq, θ, and D_{surf}.

3.2.3 *Applying the Model*

We tested the accuracy of the derived equations of motion by stiffening the track spring as much as possible and treating the system as a leg running on a non-compliant surface. This configuration was then compared to McMahon and Cheng's model (1990) by employing their inputs and attempting to reproduce their outputs. We did this by starting our model at mid-step (where more variables were known) and adjusting horizontal velocity and Y_m (hence leg compression) until their initial conditions (which are also the final conditions due to symmetry) were met. We then calculated the same output parameters and compared these to their results.

The model was also used to provide an estimate of the maximum effective track mass that could be used in the design of the track platform. As described in Chapter 2, we wanted the track platform to have a negligible effect on the system and the forces that are being recorded by the force plate. In order to do this we restricted the entire system to move in the vertical direction only to simulate mid-step (where the maximum force is produced). We kept the surface stiffness at a constant value of 100kN/m and recorded the maximum force output from the model as we increased the mass. We took the maximum track mass to be the mass at which the change in peak force output was 10% when compared to a track mass equal to 1 kg.

Lastly, the model was used to test our assumption that the leg does behave like a linear spring while running on compliant surfaces. We did this by testing how well the model matched the experimental data. All of the inputs to the model were the experimental values converted into dimensionless form: K_{LEG}, M, L_o, R, B, X_m, Y_m, U, V, and W. The initial positions were taken from the sweep angle data:

$$X_m = \sin\theta \tag{3.4}$$

$$Y_m = \cos\theta. \tag{3.5}$$

The initial velocities were estimated from the kinematic data using the same Matlab programs that were used in Chapter 2 for determining the change in velocity (Appendix B). The resulting velocity values simply represented starting points. We then iterated these initial velocity magnitudes until all of the outputs were within 5% of the experimental data (including mean U). The final values that were used for the initial velocities fell within the range found from the experimental subjects as well as from other values used in the literature for human running (He et al., 1991; McMahon and Cheng, 1990). The criterion used to assure symmetry was to take the time point when the final leg length was just slightly larger than the initial value and use this duration as the contact time. All the outputs were then calculated only over the contact time. After this was completed over all surfaces, the model was used again to predict what would have happened if K_{leg} was held constant over all surfaces. This was done to observe the sensitivity between running mechanics and K_{leg}. All inputs and initial conditions that were used in the model to reproduce the experimental data were kept the same except for K_{leg}. Instead, we held the value of K_{leg} at the stiffest surface for all surfaces to observe if the results would be markedly different from the experimental results.

3.3 Results

Our model's results fell within 2% of the McMahon and Cheng model (1990). Therefore, we concluded that our equations of motion were correct and that we could include the additional component of a compliant, vertically moving track surface to our model.

The design criterion for the maximum effective track mass was estimated by the model to be less than or equal to 17% of the mass of the runner. Given that the average mass of the runner was expected to be roughly 72kg, the track platforms were designed so that they would be less than or equal to 12kg each. This allowed for a factor of safety, because the entire mass of the track platform is larger than the effective track mass.

The model accurately reproduces the experimental data to within 5% for all output parameters. This was true for all individual subjects. Averaged data were not reproduced because averages did not necessarily produce

symmetric solutions given the inputs. Therefore, a representative subject was chosen to show the results graphically.

When K_{leg} was held at the constant value given for the 945 kN/m surface, the model was not able to reproduce the experimental data, suggesting that running mechanics is sensitive to leg stiffness. Instead, the model shows what would happen if runners did not adjust their leg stiffness to accommodate for changes in surface compliance.

The dimensionless experimental data from Chapter 2 (open squares) are plotted together with the model's dimensionless predictions (closed diamonds) over all surface compliances. A line is fitted to the model's predictions. The models' predictions for running with a constant K_{leg} over surfaces of different compliance are also shown (closed circles) to show what would be expected if K_{leg} did not adjust to accommodate changes in surface stiffness. The results show that the model could mostly predict the experimental data well if K_{leg} was adjusted to changes in surface stiffness. For example, the effective vertical stiffness was experimentally found to be constant. The model was able to produce the same result only if K_{leg} was increased on more compliant surfaces (closed diamonds). When K_{leg} did not change to accommodate changes in surface stiffness, K_{vert} decreases drastically on the more compliant surfaces (Figure 3.2).

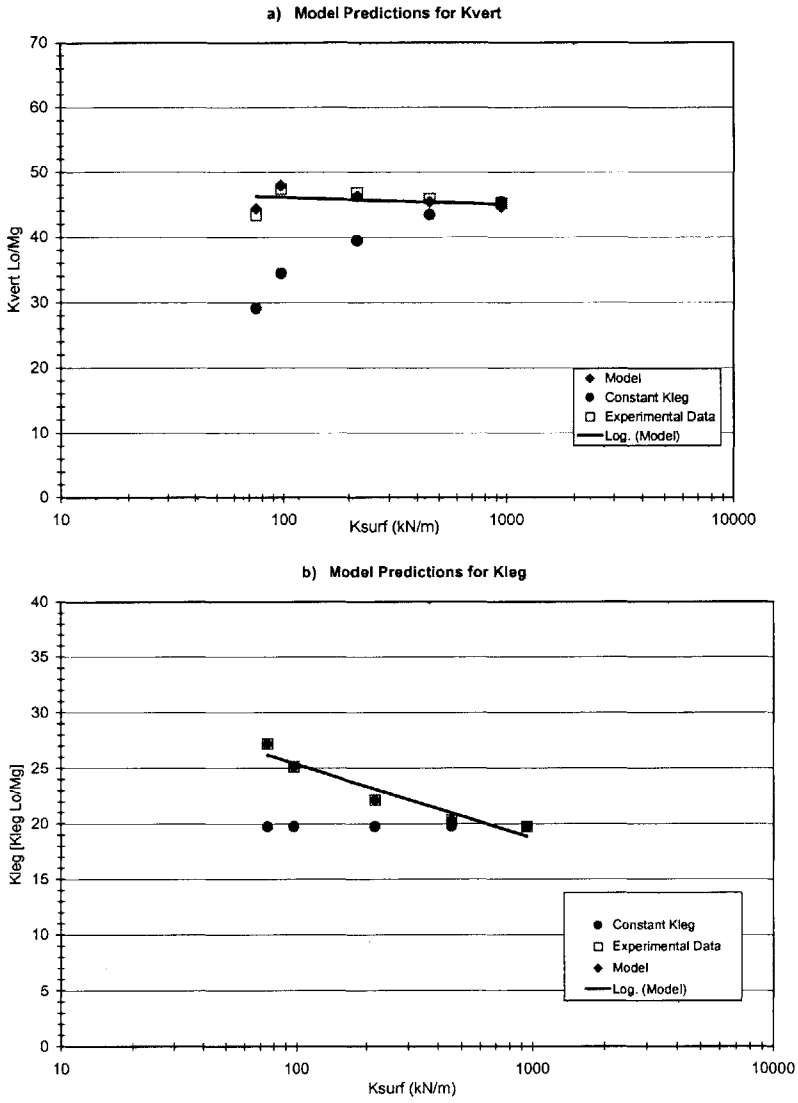

Figure 3.2: Dimensionless model predictions and experimental data for a) Kvert, and b) Kleg

Similar results can be seen when comparing other results from the experiment with model predictions. Peak vertical force, contact time, and sweep angle are tightly predicted when the model is used with a varying K_{leg}. The results diverge from the observed experimental data when a constant K_{leg} is used (Figure 3.3). Center of mass displacement is found to be constant over all surfaces both experimentally and theoretically when K_{leg} changes, but is predicted to decrease on more compliant surfaces if K_{leg} is held constant (Figure 3.4a).

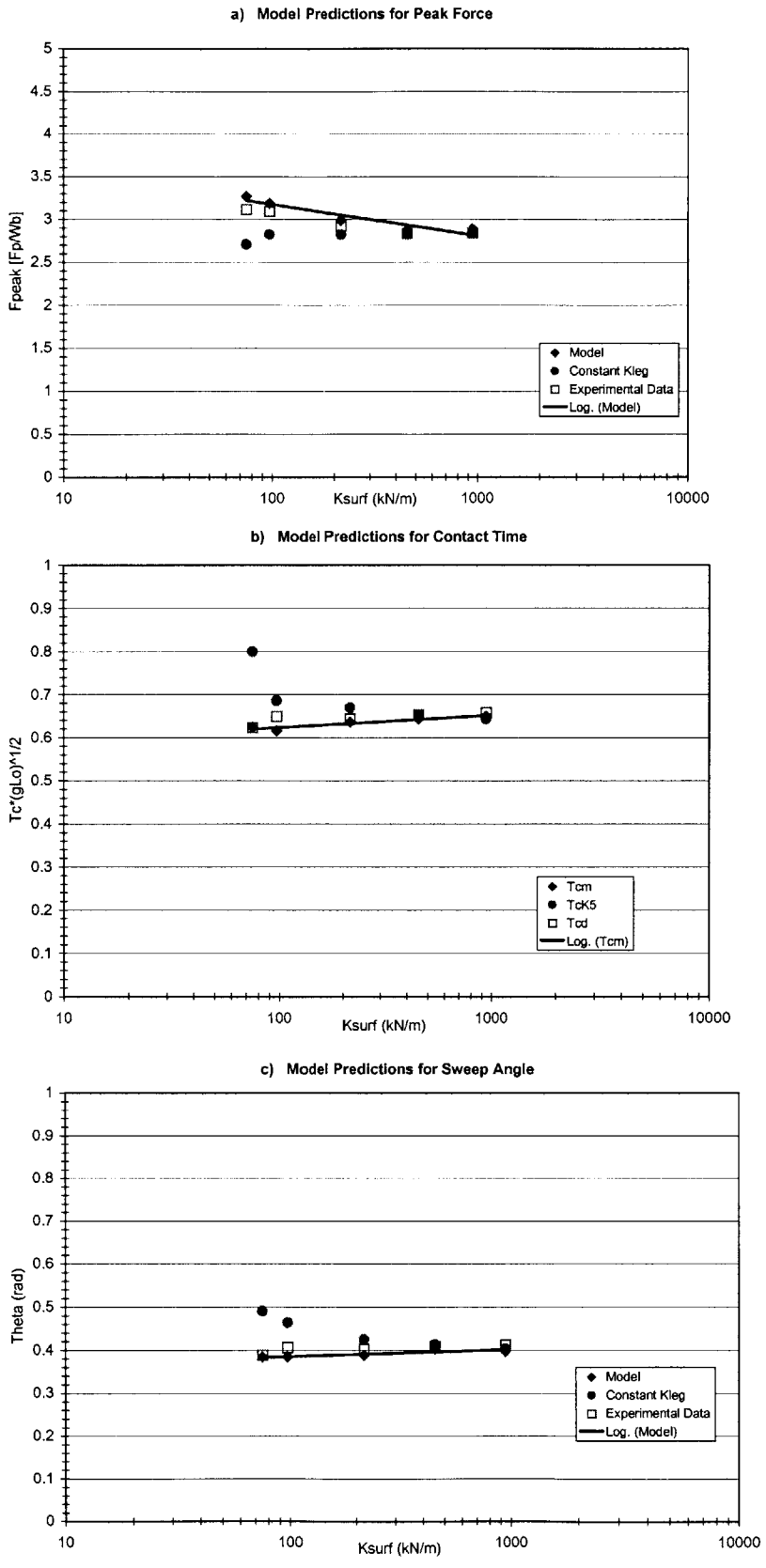

Figure 3.3: Dimensionless model predictions and experimental data for a) Peak force, b) Contact time, and c) Sweep angle

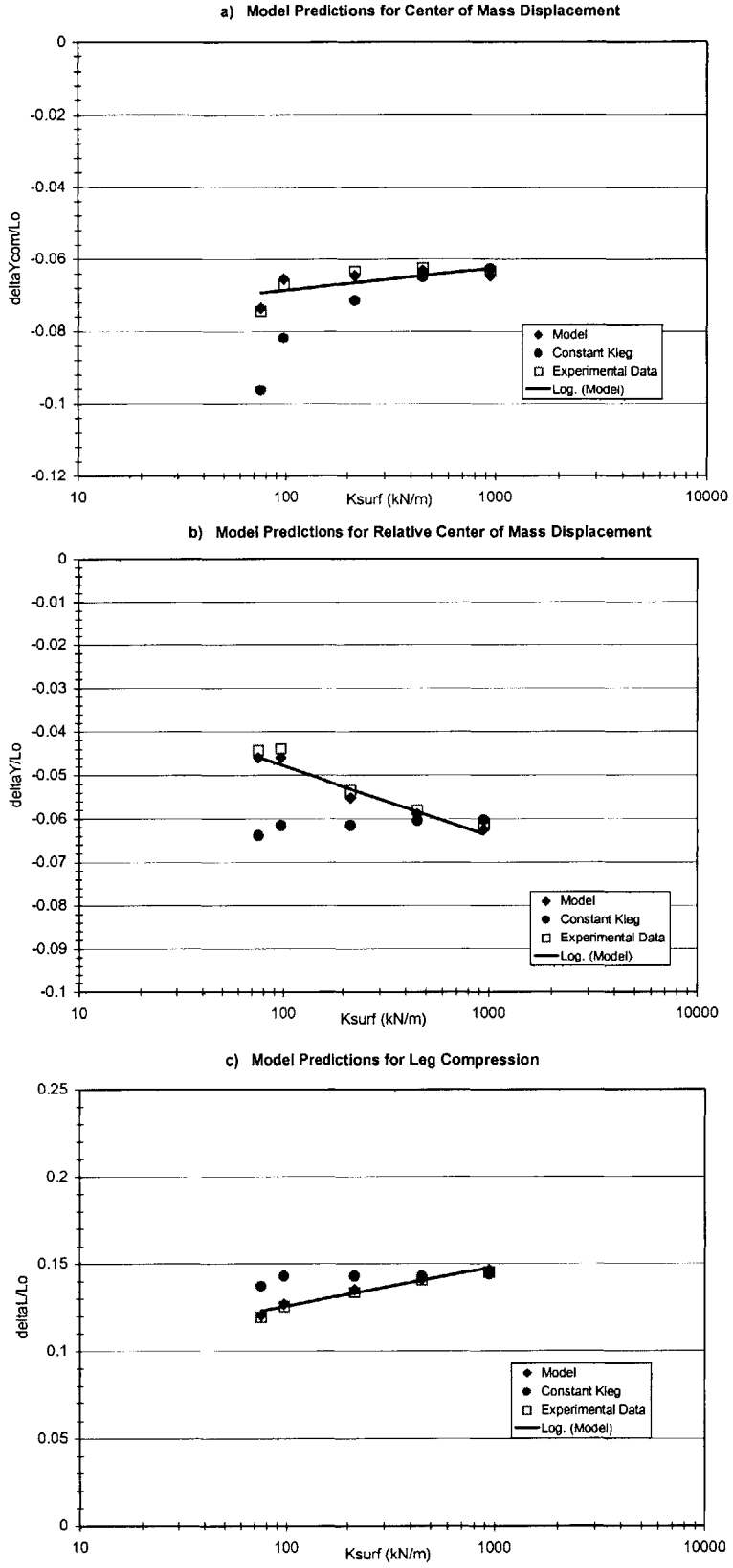

Figure 3.4: Dimensionless model predictions and experimental data for a) Center of mass displacement, b) Relative center of mass displacement, and c) Leg compression

A constant K_{leg} over all surfaces would mean that the leg would compress by the same amount on each surface contrary to what was observed experimentally (Figure 3.4 c). Because the leg maintains a constant stiffness and length while the ground surface is deflecting more on the compliant surfaces, we would expect that the relative displacement of the center of mass would remain constant as well (Figures 3.5 and 3.4 b). This is what is observed and is again contrary to what is observed experimentally and predicted theoretically when K_{leg} is allowed to change.

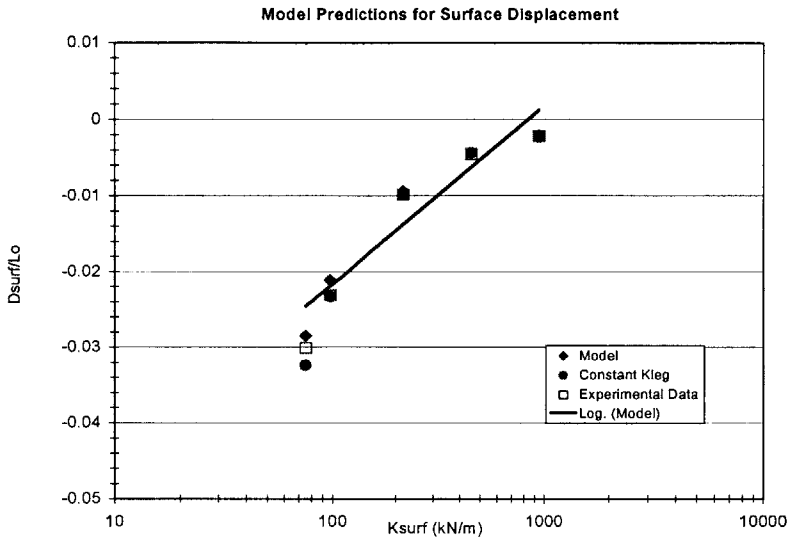

Figure 3.5: Dimensionless model predictions and experimental data for Surface displacement

We initially stated that the choice of K_{leg} was critical in maintaining stability and symmetry in the model. If K_{leg} is too soft, as it is on the more compliant surfaces, than the body rises too late and the runner would be expected to take a longer step. The model was able to predict this when K_{leg} was held constant (Figure 3.6 a).

Stride frequency, surface displacement, and mean forward velocity were not affected by K_{leg}, and both forms of the model were able to predict the experimental data well (Figures 3.5, 3.6 b and 3.7).

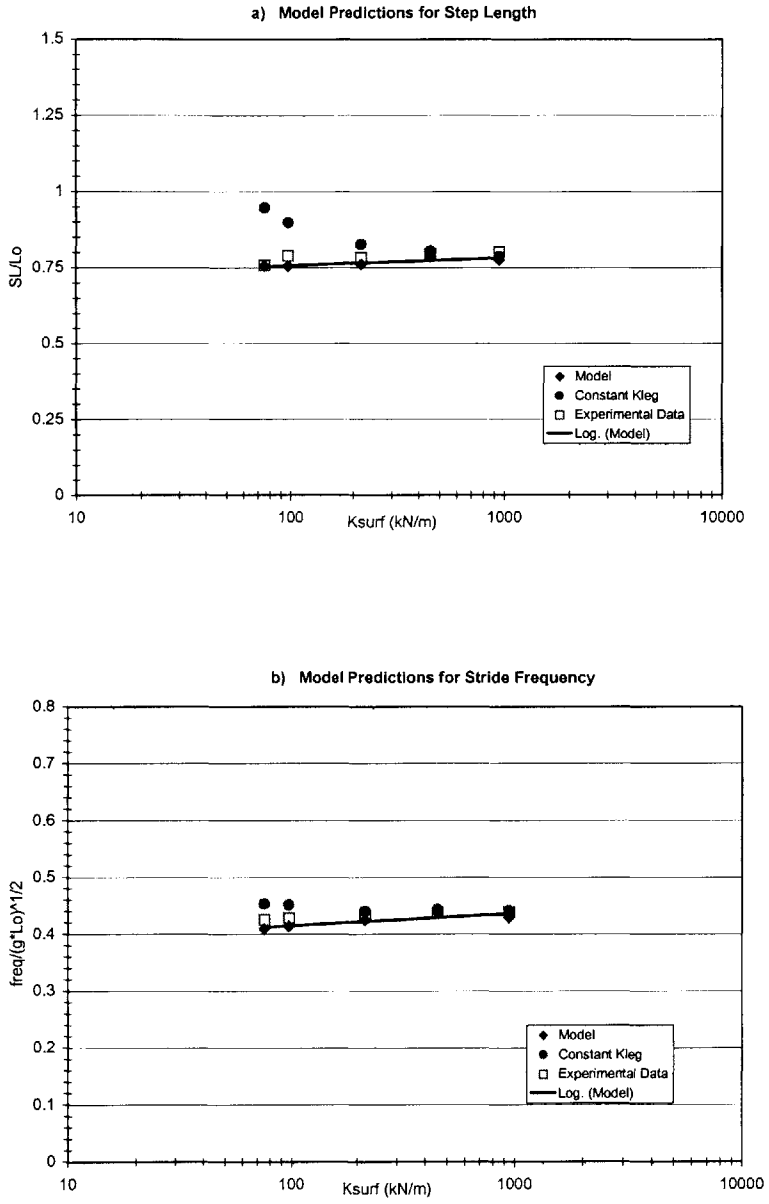

Figure 3.6: Dimensionless model predictions and experimental data for a) Step length, and b) Stride Frequency

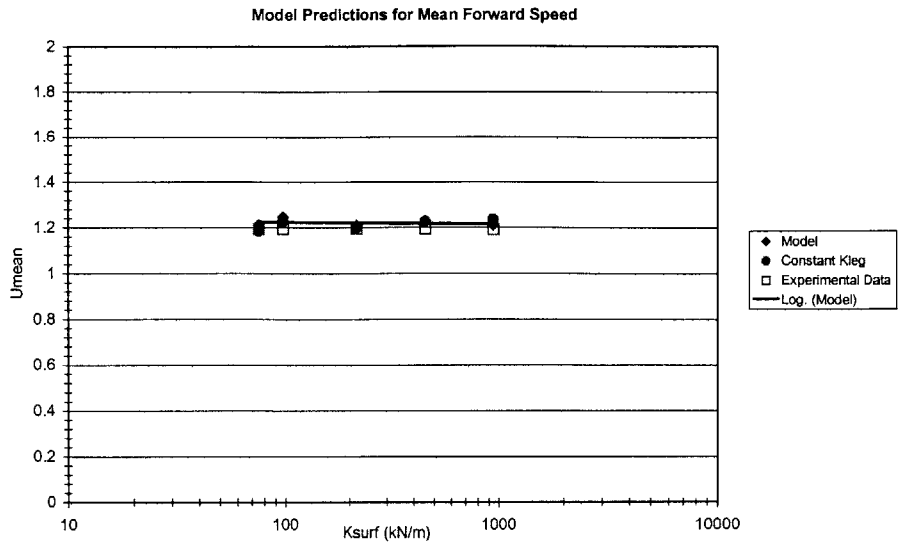

Figure 3.7: Dimensionless model predictions and experimental data for mean forward speed

Other results from the model include the center of mass trajectory as well as system energetics. The center of mass trajectory of the runner over contact time should be symmetric and also not change with surface compliance if running dynamics are to remain similar over all surfaces. The model was able to reproduce this behavior (Figure 3.8). The model was also used to calculate the energy stored in the track over dimensionless time using equation 2.21 (Figure 3.9). The change in energy (i.e. the maximum value of each curve shown) represents the amount of energy the ground surface stores during ground contact.

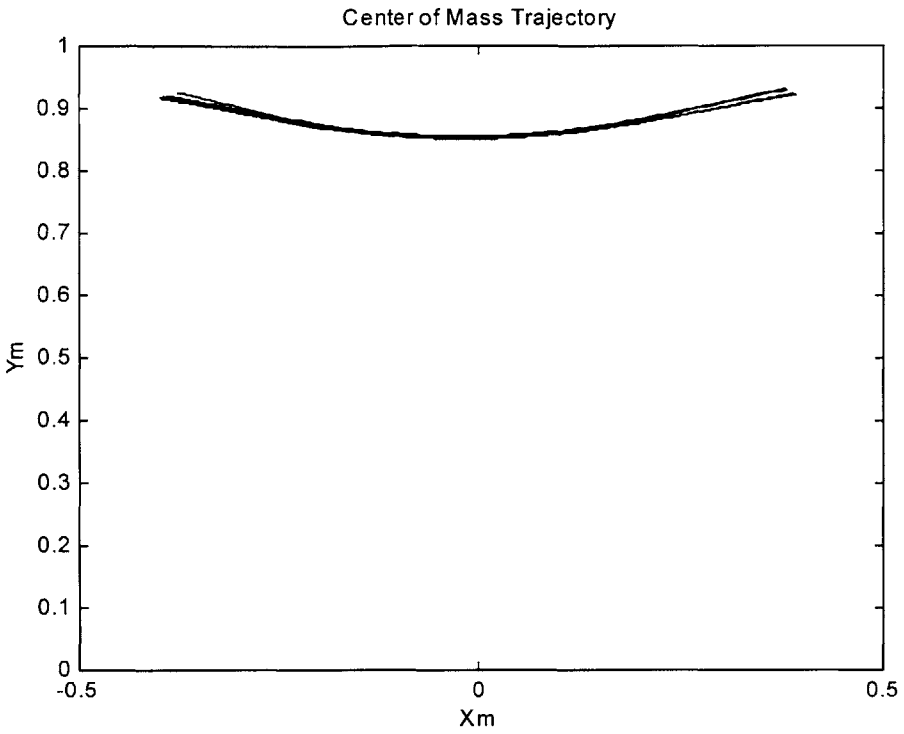

Figure 3.8: Trajectories of the model's Mm (runner's center of mass) during the time of contact (shown in dimensionless form)

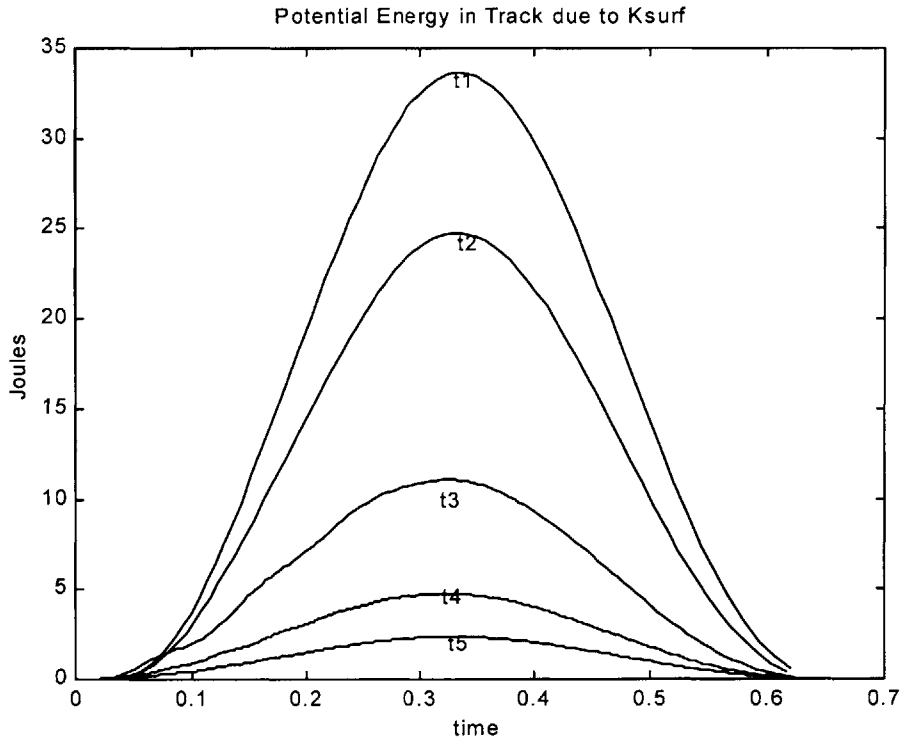

Figure 3.9: Potential track energy due to K_{surf} over dimensionless time for each surface (t1 = 76 kN/m to t5 = 945 kN/m)

The amount of energy stored by the track during ground contact as predicted from the model was plotted with the same track energy calculated directly from the experimental data (Figure 3.10). Again, the model predictions (closed diamonds) fall well within 5% of the experimental data (open squares).

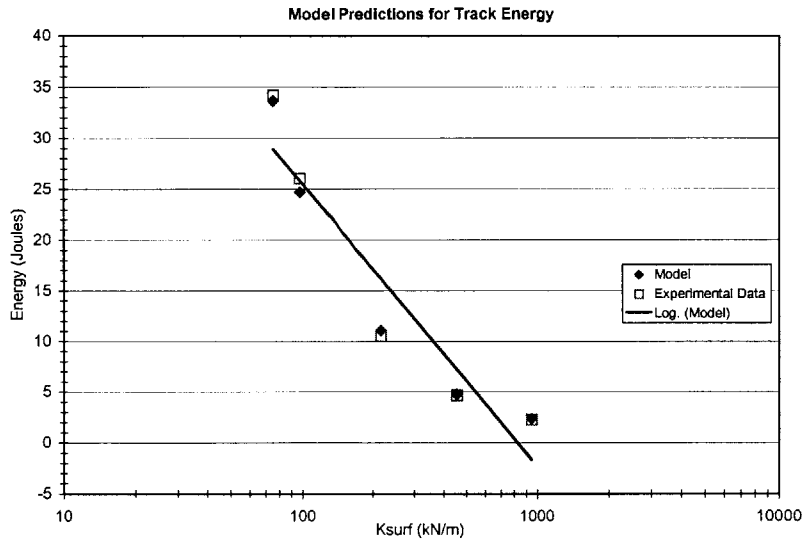

Figure 3.10: Model and experimental data for potential track energy due to K_{surf}

3.4 Discussion

We used a computer model of a simplified mass-spring system to represent a human runner in contact with a compliant surface for several reasons. Our primary goal was to test our assumption that the leg still behaves like a linear spring while running on surfaces of different compliance. The model was also used to gain a deeper understanding of how the system worked, to provide design information for the track platforms, and to predict what would happen if the runner's leg did not change stiffness to adapt to changes in surface compliance (i.e. what the sensitivity is between running mechanics and K_{leg}).

To test our linear leg spring assumption, we used inputs from the experiment conducted in Chapter 2, and compared the model's outputs to the experimental results. The results show that the model can accurately predict the experimental data to within 5%. Therefore, we conclude that the assumption that a runner's leg behaves in a similar manner to a linear spring while running over surfaces of different compliance is supported.

We also observed the results of the model when K_{leg} was not adjusted (contrary to what is obsered experimentally) for each compliant surface, and compared these results to the experimental data. A constant K_{leg}

predicted, as would be expected from Figure 2.1, that the peak force and leg compression remained constant over different surfaces (Figures 3.3a and 3.4c). We found that if K_{leg} is not adjusted, the model predicts that a runner would not maintain similar running dynamics over all surfaces as hypothesized in Chapter 2. Recall that the experimental results from Chapter 2 and the literature show that running dynamics do generally remain the same while running or hopping on surfaces of different compliance (Ferris and Farley, 1997; McMahon and Greene, 1979). Therefore, the results suggest that human runner's change their leg stiffness in order to achieve a preferred running state. In other words, running mechanics is sensitive to leg stiffness.

The model proved to be a useful tool in understanding and testing a human running on surfaces of different compliance. A simple representation of a complex system is a useful starting tool in understanding the system as a whole, but as more is learned about the basic mechanisms behind the system, new information needs to be added into the model. In the future we hope to take what we have learned and combine it with Farley et al's ideas on the mechanisms for K_{leg} adjustment to develop a more sophisticated computer simulation of human running (Farley et al., 1998; Farley and Morgenroth, 1999).

3.5 References

Cavagna, G. A., Heglund, N. C., and Taylor, C. R. (1977). Mechanical Work in Terrestrial Locomotion: Two Basic Mechanisms for Minimizing Energy Expenditure. Am. J. Physiol. *233*, R243-R261.

Farley, C. T., Houdijk, H. H. P., Strien, C. V., and Louie, M. (1998). Mechanism of Leg Stiffness Adjustment for Hopping on Surfaces of Different Stiffnesses. J. Appl. Physiol. *85*, 1044-1055.

Farley, C. T., and Morgenroth, D. C. (1999). Leg Stiffness Primarily Depends on Ankle Stiffness During Human Hopping. Journal of Biomechanics *32*, 267-273.

Ferris, D. P., and Farley, C. T. (1997). Interaction of Leg Stiffness and Surface Stiffness During Human Hopping. The American Physiological Society, 15-22.

Ferris, D. P., Liang, K., and Farley, C. T. (in press). Runners Adjust Leg Stiffness for Their First Step on a New Running Surface.

Ferris, D. P., Louie, M., and Farley, C. T. (1998). Running in the Real World: Adjusting Leg Stiffness for Different Surfaces. Proc. R. Soc. Lond. B *265*, 989-994.

He, J., Kram, R., and McMahon, T. A. (1991). Mechanics of Running Under Simulated Low Gravity. The American Physiological Society, 863-870.

McMahon, T. A. (1990). Spring-Like Properties of Muscles and Reflexes in Running. In Multiple Muscle Systems: Biomechanics and Movement Organization, J. M. Winters and S. L.-Y. Woo, eds. (Springer-Verlag), pp. 578-590.

McMahon, T. A., and Cheng, G. C. (1990). The Mechanics of Running: How does Stiffness Couple with Speed? Journal of Biomechanics *23*, 65-78.

McMahon, T. A., and Greene, P. R. (1979). The Influence of Track Compliance on Running. Journal of Biomechanics *12*, 893-904.

Chapter 4
Summary and Conclusions

4.1 Introduction

The purpose of this thesis is to explore what happens energetically and mechanically to humans as they run on surfaces of different compliance. McMahon and Greene were the first to explore the effects of surface compliance on running mechanics when they developed their tuned track in 1979. The effects of surface compliance on many of the dynamic and mechanical parameters of running and hopping have since been studied. On compliant surfaces a runner's speed enhances, athletic injury decreases, center of mass displacements are unaffected, leg and ankle stiffness increase, and limb angles straighten (Farley et al., 1998; Farley and Morgenroth, 1999; Ferris and Farley, 1997; Ferris et al., in press; Ferris et al., 1998). The kinetic and gravitational potential energies involved in running occur in phase, and the potential energy stored in the leg at mid-step has been shown to be in an elastic form which can return energy to the runner (Alexander, 1991; Cavagna et al., 1976). Therefore, a main assumption behind all of the above-mentioned findings was that the leg could be considered to behave like a linear spring. Several studies have been done in an attempt to understand this "leg spring". For instance it has been shown that during locomotion, the stiffness of the leg spring is independent of speed, decreases with knee flexion, increases with stride frequency, increases with size, and decreases with ground stiffness (Farley et al., 1993; Farley and Gonzalez, 1996; Ferris and Farley, 1997; McMahon and Cheng, 1990; McMahon et al., 1987).

The energetics of running has also been extensively studied. It is believed that animals do what they can to minimize the cost of locomotion. Most of the cost of running is from producing the forces necessary to support the weight of the runner in the amount of time available during ground contact (Kram and Taylor, 1990; Roberts et al., 1998). However, by maximizing the spring-like properties of the leg (i.e. conservative forces), animals can reduce the amount of active muscle work (i.e. non-conservative forces), and therefore conserve the amount of energy required to run (Farley et al., 1991; Roberts et al., 1997; Taylor, 1992).

This thesis is an attempt to link the energetics and mechanics of running over compliant surfaces. We further challenge the assumption that the leg behaves like a linear spring while running on surfaces of different compliance. Through experimentation and theoretical modeling, we set out to test our hypothesis that the metabolic cost of running decreases when running on compliant surfaces within the range of the tuned track, and that runners would adapt to these surfaces without altering their general running dynamics.

4.2 Experiment with Humans Running on Surfaces of Different Compliance

Chapter 2 describes the methods and accomplishments of the experiment in detail. One achievement of the experiment was the development of a running track with adjustable stiffness that was incorporated into a force plate fitted treadmill. The stiffness range of this track was from within the middle of the tuned track range (75.4 kN/m) to a stiffness of 945.7 kN/m. The experimental protocol was designed to provide force plate, kinematic, and energetic data. Our results showed that the stiffness of the leg spring did increase when running on more compliant surfaces. We also showed that the metabolic cost of running, as well as the cost coefficient, decreased with a 12-fold reduction in surface stiffness. The other parameters measured were unaffected by surface stiffness and therefore we can conclude that the overall running dynamics remain similar over all surfaces.

4.3 Modeling the Leg Spring on a Compliant Surface

The model in Chapter 3 was used to test our assumption that the leg behaves as a linear spring while running on compliant surfaces. The theoretical model's results were within 5% of the experimental results, thus supporting our leg spring assumption. We also used the model to study the effects on running if the stiffness of the leg spring was not adjusted to adapt to changing surface stiffnesses. The results showed clear changes in contact time, stride frequency, sweep angle, and other parameters. The observed changes suggest that a change in overall running dynamics occur as a result of not adjusting K_{leg} on compliant surfaces. As shown in Chapter 2, there is experimental evidence that runners maintain similar running dynamics over all surfaces studied. Therefore, the model supports the findings that the leg stiffness must adapt to changes in surface stiffness in an attempt to maintain consistent running dynamics over different surfaces.

4.4 Discussion

The experimental and theoretical results of this thesis support the hypothesis that the metabolic cost of running is decreased and that running dynamics are unaffected when running on compliant surfaces within the range of the tuned track. We observed a 12% reduction in metabolic cost over a 12-fold change in surface stiffness. In Chapter 2 we discussed possible explanations for the decrease in metabolic energy. We entertained the idea of the leg spring and the track spring working together to reduce fluctuations in total mechanical energy of the runner's center of mass while maintaining a constant overall stiffness. If we could have measured the actual strain of the muscle, we could have observed the changes in the tendons and the muscles directly. By doing so we might be able to determine if the observed decrease in work is due to the tendons (conservative forces) working more than the muscle bellies (non-conservative forces), or if perhaps the muscles operate more isometrically, while running on the more compliant surfaces. We also showed that the track was able to store and return up to 26% of the energy required to move the center of mass of the runner during a step. However, we were unable to determine if the track actually returned this energy to the runner.

In order to explore the mechanisms for the observed changes in metabolic energy, additional studies need to be done. Expanding the range of surface stiffnesses beyond what was studied in this thesis would perhaps provide a true minimum in the metabolic reduction as well as some information on the control mechanisms behind the stability of running on different surfaces. Another interesting study would involve studying running on surfaces encountered in the real world such as sod, sand, and clay and observing the metabolic and mechanical effects of the runner in these situations.

Also, as described in Chapter 3, the mass-spring model could be used to predict the total mechanical energy on the center of mass of the runner. A model that fit the experimental data more tightly might be able to uncover the reason for the reduced metabolic energy by examining each aspect of the total mechanical energy of the center of mass in detail.

Both the experimental and theoretical results support the observation that runner's change their leg spring stiffness in an attempt to not disrupt their overall running dynamics. Researchers have commented that an observer only looking at the upper body of a runner should not be able to tell when the runner experiences a change in ground stiffness (Ferris et al., in press; McMahon and Greene, 1979). Therefore this result may be a general principle of running. It is believed that the adjustment in leg stiffness is an attempt to keep the overall stiffness of the system (runner and ground) constant. Studies have been done that suggest that the mechanism for K_{leg} adjustment is primarily due to changes in ankle stiffness and limb geometry (Farley and Morgenroth, 1999; Ferris et al., 1998). However, the underlying control mechanisms of the K_{leg} adjustment are still not clearly understood. Lastly, can a clear link be made between the reduction in metabolic cost and this mechanical consequence?

A universal goal in studying biomechanics is to understand the basic control mechanisms that govern animal locomotion. We believe that the results of this thesis bring researchers one step closer to addressing this challenge by attempting to link the empirical relationships of human running. Through applying what we and others have learned thus far to develop computer simulations of a moving animal, we believe that the apparently complex mechanisms of locomotion can be broken down into a basic structure relying on simple principles. In an attempt to this end, a computer simulation of a running biped (RUBI) is being developed at the Massachusetts Institute of Technology's Leg Laboratory. The intention of this project is to develop a physiologically accurate and stable mathematical model of a running biped that can handle blind disturbances (such as changes in surface stiffness) without having to alter its basic control mechanisms. We hope to use this model (which has just achieved its first stable generation) to help determine what aspects of running are fundamental and what parameters are derived (a dynamical consequence).

Through the use of mathematical computer simulations, as well as results from experimentation similar to the work done in this thesis, a deeper understanding of the basic control mechanisms involved in human running and animal locomotion can be obtained. The applications of such information are limitless. Two major applications would be in the advancement of robotics and prosthetics. A robot that could move smoothly and gracefully without consuming a lot of energy would benefit many, if not all, industries. Lower leg amputees would also benefit greatly from this and related work. Without leg springs, amputees on artificial legs consume a lot of energy during locomotion. If the artificial leg and its joints sensed changes in surface conditions and adjusted its properties similar to what is observed experimentally and shown theoretically, amputees would be able to move in a more natural and stable manner while conserving energy.

4.5 References

Alexander, R. M. (1991). Energy-Saving Mechanisms in Walking and Running. Journal of Experimental Biology *160*, 55-69.

Cavagna, G. A., Thys, H., and Zamboni, A. (1976). The Sources of External Work in Level Walking and Running. J. Physiol. Lond. *262*, 639-657.

Farley, C. T., Blickman, R., Saito, J., and Taylor, C. R. (1991). Hopping Frequency in Humans: A Test of How Springs Set Stride Frequency in Bouncing Gaits. the American Physiological Society, 2127-2132.

Farley, C. T., Glasheen, J., and McMahon, T. A. (1993). Running Springs: Speed and Animal Size. Journal of Experimental Biology *185*, 71-86.

Farley, C. T., and Gonzalez, O. (1996). Leg Stiffness and Stride Frequency in Human Running. Journal of Biomechanics *29*, 181-186.

Farley, C. T., Houdijk, H. H. P., Strien, C. V., and Louie, M. (1998). Mechanism of Leg Stiffness Adjustment for Hopping on Surfaces of different Stiffnesses. J. Appl. Physiol. *85*, 1044-1055.

Farley, C. T., and Morgenroth, D. C. (1999). Leg Stiffness Primarily Depends on Ankle Stiffness During Human Hopping. Journal of Biomechanics *32*, 267-273.

Ferris, D. P., and Farley, C. T. (1997). Interaction of Leg Stiffness and Surface Stiffness During Human Hopping. The American Physiological Society, 15-22.

Ferris, D. P., Liang, K., and Farley, C. T. (in press). Runners Adjust Leg Stiffness for Their First Step on a New Running Surface. .

Ferris, D. P., Louie, M., and Farley, C. T. (1998). Running in the Real World: Adjusting Leg Stiffness for Different Surfaces. Proc. R. Soc. Lond. B *265*, 989-994.

Kram, R., and Taylor, C. R. (1990). Energetics of Running: a New Perspective. Nature *346*, 265-267.

McMahon, T. A., and Cheng, G. C. (1990). The Mechanics of Running: How does Stiffness Couple with Speed? Journal of Biomechanics *23*, 65-78.

McMahon, T. A., and Greene, P. R. (1979). The Influence of Track Compliance on Running. Journal of Biomechanics *12*, 893-904.

McMahon, T. A., Valiant, G., and Frederick, E. C. (1987). Groucho Running. J. Appl. Physiol. *62*, 2326-2337.

Roberts, T. J., Kram, R., Weyand, P. G., and Taylor, R. (1998). Energetics of Bipedal Running I. Metabolic Cost of Generating Force. The Journal of Experimental Biology *201*, 2745-2751.

Roberts, T. J., Marsh, R. L., Weyand, P. G., and Taylor, C. R. (1997). Muscular Force in Running Turkeys: The Economy of Minimizing Work. Science *275*, 1113-1115.

Taylor, R. C. (1992). Cost of Running Springs. In Physiological Adaptions in Vertebrates: Respiration, Circulation, and Metabolism, S. C. Wood, R. E. Weber, A. R. Hargens and R. W. Millard, eds. (New York: Marcel Dekker, Inc.), pp. 55-65.

Appendix A

The following Matlab (version 4.0) programs were written and used to calculate the knee angle of the runner at mid-step. The output plots are displayed after the code and are of a representative subject for one run: SR at 216 kN/m stiffness.

Running.m

```
% this program results in: putting mac reflex data into matrixform,
% plotting data, plotting data over time, picking the min. point
% so knee angle can be calculated

function running()

% input necessary data per file doing here
filename = 'sr-3-1.tsv';
frames = 600;
markers = 5;
cal1 = [20361 10573];    % x1, y1, in pixels
cal2 = [9654 10677];     % x2, y2, in pixels
callength = 0.96;        % [m]
speed = 3.93;            % [m/s]

% calls readfile to convert data to matrix form, outputs 3 matrices: #,x,y
[frameNo, x, y] = ReadFile(filename, frames, markers);

%calibration length (pixels to m)
scale = callength/sqrt((cal1(1)-cal2(1))^2+(cal1(2)-cal2(2))^2);
x = x*scale;
y = -y*scale;

%plots data as see it in maxdos, to make sure matrices converted OK
plot(x(:,1),y(:,1),'ro',x(:,2),y(:,2),'bo',x(:,3),y(:,3),'go')
title('Mac Reflex data over 10 sec')
axis([0.25 2.5 -2.5 0.25])
axis equal
pause
```

```
% to see data spread out over time (xprime), use calibrated length
for i = 1:frames
  xprime(i,:) = x(i,:)-speed*i/60;
end

plot(xprime(:,1),y(:,1),'ro',xprime(:,2),y(:,2),'bo',xprime(:,3),y(:,3),'g
o')

axis([-40 5 -1.6 -0.2])
title('<- = dir of 10 sec run, X vs Y data for hip (red), knee (blue) and
ankle')

xlabel(['X (m)']); ylabel(['Y (m)']);

% Select Hip points.

for j=1:10
  zoom on
  fprintf('\n min Hip point:\n')
  input('Zoom in/out until ready to select a point.\nThen press return.')
  fprintf('Select point.\n')
  [xinput,yinput] = ginput(1);

  % Find match in experimental data.

  dx = xprime(:,1)-xinput;
  dy = y(:,1)-yinput;
  for i = 1:frames
   delta(i) = sqrt(dx(i)^2+dy(i)^2);
  end

  [minimum Iinput(j)] = min(delta);
  [minimum Imin] = min(y(Iinput(j)-10:Iinput(j)+10,1));
  Iinput(j) = Iinput(j)-10+Imin-1;
  xinput = xprime(Iinput(j),1);
  yinput = y(Iinput(j),1);
```

```
  % Mark point on graph and print position.

  line([xinput xinput],[-2 0])
  zoom out
  pause
end

fprintf('\nAre you done?\nIf yes, press return.\n')
pause
zoom off

% display frame numbers from above point picking and print only those
%frames for hip, knee, and ankle

fprintf('Frame numbers for mid step point of 10 steps =')
Iinput

% spread out plot

plot(xprime(Iinput,1),y(Iinput,1),'ro',xprime(Iinput,2),y(Iinput,2),'bo',x
prime(Iinput,3),y(Iinput,3),'go')
title('Mid Step points for hip knee and ankle')
axis equal
pause

%collapsed plot corrected for front/back movement (i.e. horizontal hip
movement)

diff = x(Iinput(1),1) - x(Iinput,1);
for i = 1:3
  xcol(:,i) = x(Iinput,i) + diff;
end

plot(xcol(:,1),y(Iinput,1),'ro',xcol(:,2),y(Iinput,2),'bo',xcol(:,3),y(Iin
put,3),'go')
title('Collapsed plot of hip, knee, and ankle, to see variation')
axis equal
pause
```

```
% Calculate the leg angles

for i=1:10
  uleg(i,:)=[(x(Iinput(i),1)-x(Iinput(i),2)) (y(Iinput(i),1)-
y(Iinput(i),2))];
  lleg(i,:)=[(x(Iinput(i),3)-x(Iinput(i),2)) (y(Iinput(i),3)-
y(Iinput(i),2))];

  ulegM(i)=(sqrt((x(Iinput(i),2)-x(Iinput(i),1))^2+(y(Iinput(i),2)-
y(Iinput(i),1))^2));
  llegM(i)=(sqrt((x(Iinput(i),3)-x(Iinput(i),2))^2+(y(Iinput(i),3)-
y(Iinput(i),2))^2));


theta(i)=acos((dot(uleg(i,:),lleg(i,:)))/(ulegM(i)*llegM(i)))*180/3.14159;
end

fprintf('Mid stance leg angle for 10 steps')
theta
fprintf('Average leg angle for 10 steps')
Avg_Theta = sum(theta)/10
```

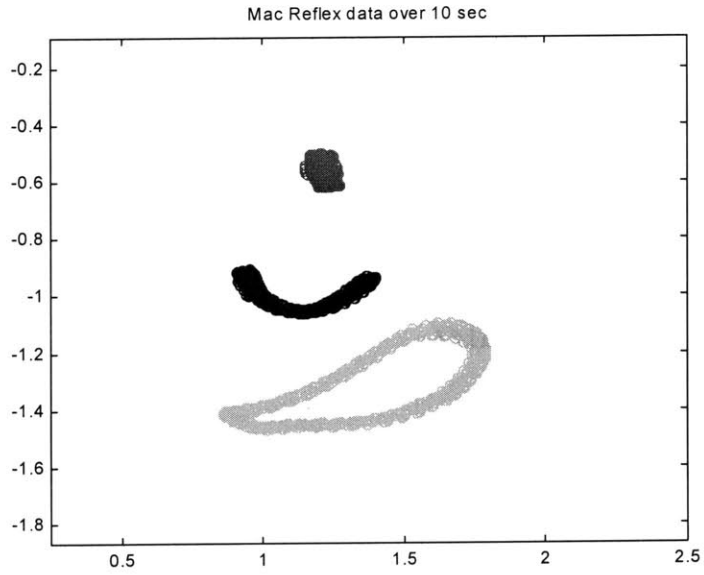

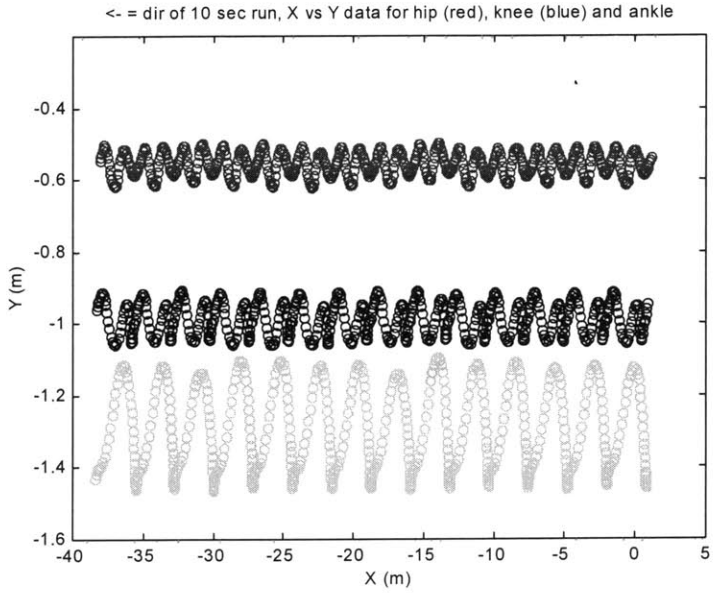
<- = dir of 10 sec run, X vs Y data for hip (red), knee (blue) and ankle
-0.4
-0.6
-0.8
-1
-1.2
-1.4
-1.6
Y (m)
-40
-35
-30
-25
-20
-15
-10
-5
0
5
X (m)

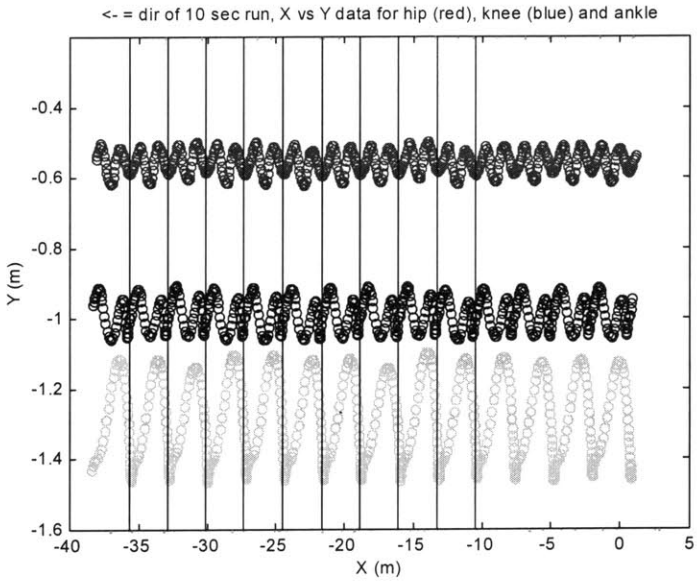
<- = dir of 10 sec run, X vs Y data for hip (red), knee (blue) and ankle
-0.4
-0.6
-0.8
-1
-1.2
-1.4
-1.6
Y (m)
-40
-35
-30
-25
-20
-15
-10
-5
0
5
X (m)

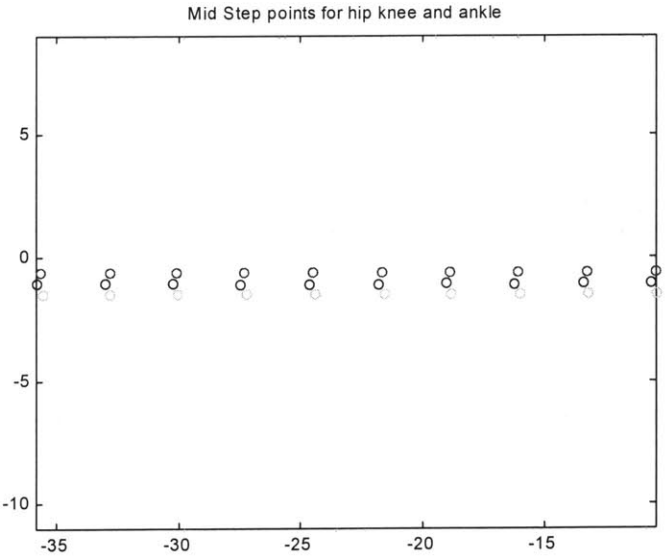
Mid Step points for hip knee and ankle
5
0
-5
-10
-35
-30
-25
-20
-15

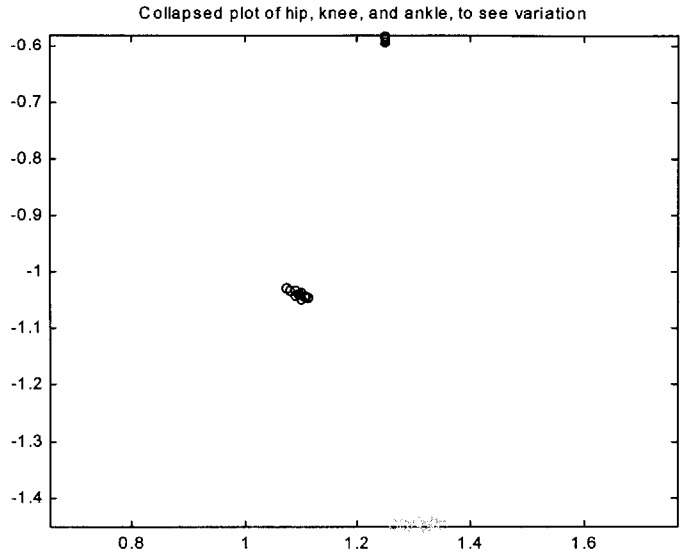

Readfile.m

```
function [frameNo, x, y] = ReadFile(filename, frames, markers)

% Open the file and store its content into column(frame #, 2 * markers+1).
fid = fopen(filename);

for i = 1:frames
   row(1,i) = fscanf(fid, '%g', [1, 1]);  % Read the frame number.
   j = 2;
      while j < 2 * markers + 2           % Read the position of each
                                             marker for this frame.
      position = ftell(fid);
      char = fscanf(fid, '%c%c%c', [2,1]);
      if char(2) == '   '                 % If no marker for this frame
         row(j:j+1,i) = [NaN NaN]';       % enter NaN for x and y.

      else                                % Else enter x and y position.
         status = fseek(fid, position, 'bof');
         row(j:j+1,i) = fscanf(fid, '%g %g', [2, 1]);
      end
      j = j + 2;
   end
end

column = row';    % Frame number and x and y for each marker in columns.
fclose(fid);
```

```
frameNo=column(:,1);            % Store frame numbers in FrameNo.
for i = 1:markers-2             % Store each marker's x and y position
   x(:,i)=column(:,i*2);        % in x(frame #, marker #) and
   y(:,i)=column(:,i*2+1);      % y(frame #, marker #) respectively.
end
```

Appendix B

The following Matlab (version 4.0) program was used to estimate the change in vertical and horizontal velocities of the center of mass. The hip marker was assumed to be equivalent to the center of mass. The program takes in data from the macreflex analysis and outputs plots of the hip marker's y position and vertical velocity verses time. The x position is done in an identical manner, therefore just the y position program and output are shown here. The Readfile.m program can be found in Appendix A.. The plot is a sample of the output for the 76kN/m surface from the vert.m program. The center-line is the position data and the larger lines are the velocity data.

Vertv.m

```
%function vertv()

% input necessary data per file doing here
filename ='pgw-5-1.tsv';
frames = 600;
markers = 5;
cal1 = [19802 10565]; % x1, y1, in pixels
cal2 = [9102 10662];  % x2, y2, in pixels
callength = 0.96;     % [m]
speed = 3.7;          % [m/s]

% calls readfile to convert data to matrix form, outputs 3 matrices: #,x,y
[frameNo, x, y] = ReadFile(filename, frames, markers);

%calibration length (pixels to m)
scale = callength/sqrt((cal1(1)-cal2(1))^2+(cal1(2)-cal2(2))^2);
xpos = x*scale;
ypos = -y(:,1)*scale+0.7;
t = frameNo/60;

% Matlab's spline program, get velocities from position

% Spline positions
pp = spline(t,ypos);
xi = (0:0.001:5);
yi = ppval(pp,xi);

%calculate derivatives, velocity only
ppd = mmspder(pp);
yyd = ppval(ppd, xi);

%plot output
%plot(xi,yi,'k-', xi,yyd,'b-')
plot(xi,yyd,'k-')
OUT = [xi' yi'];
```

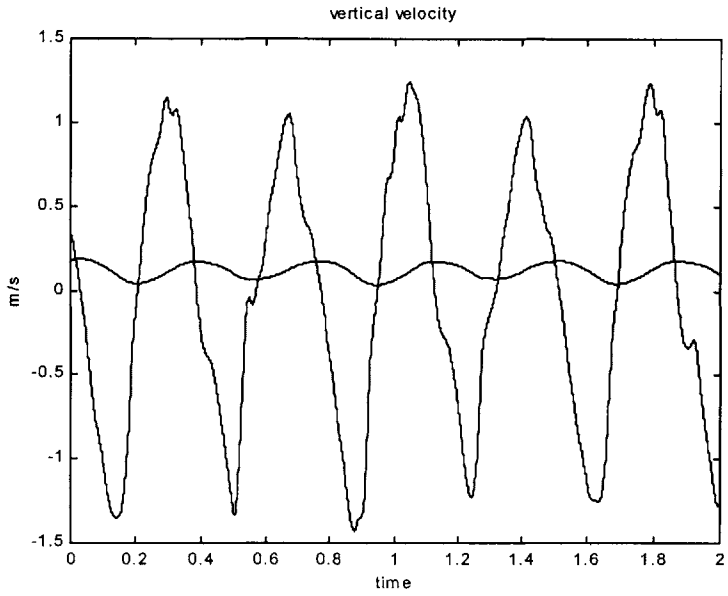
vertical velocity
1.5
1
0.5
0
-0.5
-1
-1.5
m/s
0
0.2
0.4
0.6
0.8
1
1.2
1.4
1.6
1.8
2
time

Appendix C

In Chapter 3, the three equations of motion that described the mass-spring model's configuration were presented. The derivation of these equations using Newtonian dynamics and their conversion into dimensionless form are presented here.

Dividing the system into two separate masses and drawing the free-body diagrams of the forces on these two masses defined the three equations of motion. The runner's mass was allowed to move in both the x-and y-directions. We used Newton's second law and summed the forces in both directions to obtain two of the equations of motion.

Summing the forces on the runner's mass in the x-direction gave:

$$\sum F_x = ma_x \tag{C.1}$$

$$M_m \ddot{x}_m = F_{leg} \sin\theta \tag{C.2}$$

where

$$F_{leg} = K_{leg}\left(L_o - \left((y_m - y_t)^2 + x_m{}^2 \right)^{1/2} \right). \tag{C.3}$$

Therefore, the final equation of motion defining the runner's mass in the x-direction is

$$M_m \ddot{x}_m = K_{leg}\left[L_o - \left((y_m - y_t)^2 + x_m{}^2 \right)^{1/2} \right] \sin\theta. \tag{C.4}$$

Equation C.4 is then converted into dimensionless form using the following dimensionless variables,

$$X_m = \frac{x_m}{L_o} \tag{C.5}$$

$$Y_m = \frac{y_m}{L_o} \tag{C.6}$$

$$Y_t = \frac{y_t}{L_o} \tag{C.7}$$

$$K_{LEG} = \frac{K_{leg} L_o}{M_m g} \tag{C.8}$$

$$M = \frac{M_m}{M_t} \tag{C.9}$$

$$T = t\left(\frac{g}{L_o}\right)^{1/2}. \tag{C.10}$$

The dimensionless form of the equation of motion in the x-direction for the runner's mass then becomes,

$$\frac{d^2 X_m}{dT^2} + K_{LEG}\left[1 - \left((Y_m - Y_t)^2 + X_m^2\right)^{1/2}\right]\sin\theta = 0 \tag{C.11}$$

which is the same as equation 3.1.

Summing the forces on the runner's mass in the y-direction gives:

$$\sum F_y = ma_y \tag{C.12}$$

$$M_m \ddot{y}_m = F_{leg}\cos\theta - M_m g\,. \tag{C.13}$$

Substituting in equation C.3 for F_{leg} results in the final equation of motion for the runner in the y-direction:

$$M_m \ddot{y}_m = K_{leg}\left(L_o - \left((y_m - y_t)^2 + x_m{}^2\right)^{1/2}\right)\cos\theta - M_m g\,. \tag{C.14}$$

Converting equation C.14 into dimensionless form using the variables provided in equations C.5 through C.10 derives equation 3.2 given in Chapter 3,

$$\frac{d^2 Y_m}{dT^2} - K_{LEG}\left[1 - \left((Y_m - Y_t)^2 + X_m^2\right)^{1/2}\right]\cos\theta + 1 = 0\,. \tag{C.15}$$

The track mass was restricted to move only in the y-direction. We again used Newton's second law and summed the forces in the y-direction (as in C.12) to obtain the third and final equation of motion for the mass-spring model,

$$M_t \ddot{y}_t = -K_{surf} y_t - B\dot{y}_t - M_t g - K_{leg}\left(L_o - \left((y_m - y_t)^2 + x_m{}^2 \right)^{1/2} \right) \cos\theta . \qquad \text{(C.16)}$$

Again, using the variables in equation C.5 through C.10, as well as the following dimensionless variables,

$$R = \frac{K_{surf}}{K_{leg}} \qquad \text{(C.17)}$$

$$W = \frac{w_z}{(gL_o)^{1/2}} \qquad \text{(C.18)}$$

$$B = \frac{b}{M_t \left(\frac{g}{L_o} \right)^{1/2}}, \qquad \text{(C.19)}$$

we derived the dimensionless form of the final equation of motion due to the track mass in the y-direction (3.3) as,

$$\frac{d^2 Y_t}{dT^2} + BW + RK_{LEG} MY_t + K_{LEG}\left[1 - \left((Y_m - Y_t)^2 + X_m^2 \right)^{1/2} \right] \cos\theta + 1 = 0 . \qquad \text{(C.20)}$$

Therefore, equations C.11, C.15, and C.20 are the three dimensionless equations used in the mass-spring model for Chapter 3. All variables are defined in the nomenclature.

Appendix D

The following two Matlab (version 4.0) programs are the ones that constitute the mass-spring model of Chapter 3. The first (T1_general) is the general code where the initial conditions are defined, the equations of motion are called, and the desired output is calculated for the softest surface stiffness configuration. The second program (eqm_damped) defines and solves the equations of motion.

T1_general.m

```
% code for setting up model's equations of motion at 3.7m/s
% using representive human data (PGW), T1 (75.426 kN)
global LO M KLEG R G B
LO = 0.98;          % leg length, [m]
M = 10.5778;        % dimless mass = man mass/track mass
KLEG = 27.1812;     % dimless KLEG = kleg*lo/Mg
R = 3.8091;         % dimless KSURF = Ksurf/Kleg
G = 9.81;           % gravity, [m/s] not needed in dimless
B = 45;             % damping coefficient, dimless = B/mt(g/lo)^1/2

tspan = [0 0.7];                                    % time for calcuation
yo=[-0.3794; 0.9253; 0.0; 1.165; -0.3225; 0.0]; % initial conditions: XM,
YM, YT, U, V, W
[t,y]=ode45('eqm_damp', tspan, yo);       % performs ODE(Runge
                                    Kutta)passing tspan and yo into
                                    eqm.code

for i = 1:length(t)
   theta(i) = atan(y(i,1)/(y(i,2)-y(i,3)));     % 1/2 sweep angle
   legl(i) = sqrt((y(i,2)-y(i,3))^2 + y(i,1)^2);% actual dimless leglength
   del_y(i) = (y(i,2)-y(i,3))-y(1,2);           % rel. disp of Ym wrt Yt
   disp(i) = y(i,2)-y(1,2);                     % total disp of c.o.m.,
                                                Ym-Yminit
   del_l(i) = 1*(1-legl(i));                    % change in leg length
   fy(i) = KLEG*del_l(i)*cos(theta(i));         % dimensionless vert force
end

last=min(find(legl>1.001));

kmv=72.775*G*LO*(0.5*(y(:,4).^2+y(:,5).^2));    % mass kinetic energy
umk=72.775*G*LO*0.5*KLEG*(transpose(del_l).^2); % mass potential energy
umg=72.775*G*LO*(y(:,2));                       % mass grav. Pot. energy
ktv=(72.775/M)*G*LO*(y(:,6).^2);                % track kinetic energy
utk=72.775*G*LO*0.5*R*KLEG*(y(:,3).^2);         % track potential energy
utg=(72.775/M)*G*LO*(y(:,3));                   % track grav. Pot. energy

Etot = kmv + umk + umg + ktv + utk + utg;       % total mechanical energy
Ecom = kmv +umk +umg;                           % com total energy
Esurf_tot = ktv +utk +utg;                      % track energy

dmls_legli = legl(1);                           % leglength
dmls_leglf = legl(last);
```

```
kvert = max(fy)/abs(min(disp));      % defined at mid step only!
kleg = max(fy)/(max(del_l));

Fp = max(fy);                        % Peak vertical force

Sl = 2*(y(last,1));                  % dimless step length, 2Xm

tc = Sl/mean(y(1:last,4));           % dimless contact time, Sl/U
tc_last = t(last);

dL = max(del_l);                     % spring compression at mid step

dy = min(del_y);                     % delta Y defined at midstep only!

Disp = min(disp);                    % com vertical displacmenet

ta = 2*(y(last,5));                  % ta = 2V
df = tc/(ta + tc);                   % duty factor

freq = 1/(2*(tc+ta));                % stride freq

thetai = theta(1);                   % sweep angle
thetaf = theta(last);

Uavg=mean(y(1:last,4));              % mean horizontal velocity

Vavg=mean(y(1:last,5));              % mean vertical velocity

Dsurf = min(y(:,3));                 % track deflection
Dsurf_calc = min(disp)-min(del_y);
```

eqm_damp.m

```
% code for the dimensionless equations of motion for model at 3.7 m/s
% see target_damp.m for inital conditions etc.

function primes = eqm_damp(t,y);     % takes in tspan,yo, passes out primes

global LO M KLEG R G B               % defined in set_up

theta = atan(y(1)/(y(2)-y(3)));

% equations of motion: U', V', W', U", V", W"
y1prime = y(4);
y2prime = y(5);
y3prime = y(6);
y4prime = -KLEG*(1-sqrt((y(2)-y(3))^2 + y(1)^2))*sin(theta);
y5prime = KLEG*(1-sqrt((y(2)-y(3))^2 + y(1)^2))*cos(theta)-1;
y6prime = -R*KLEG*M*y(3)-B*y(6)-KLEG*M*(1-sqrt((y(2)-y(3))^2 +
            y(1)^2))*cos(theta)-1;

primes = [y1prime; y2prime; y3prime; y4prime; y5prime; y6prime];
```


5,230-38